# PERFORMANCE EVALUATION OF OFDM SYSTEMS USING BLIND PHASE NOISE COMPENSATION IN THE PRESENCE OF JAMMER NOISE

*A Dissertation Submitted in Partial Fulfillment of the Requirement for the Award of the Degree of*

MASTER OF ENGINEERING

In Wireless Communication

Submitted By

JASON PREET KAUR

801563009

Under Supervision of

**Dr. Amit Kumar Kohli**
Associate Processor, ECED, TU

ELECTRONICS AND COMMUNICATION ENGINEERING DEPARTMENT
THAPAR UNIVERSITY, PATIALA, PUNJAB, INDIA
JUNE, 2017

# DECLARATION

I, **Jason Preet Kaur**, hereby declare that the thesis entitled "**Performance Evaluation of OFDM Systems Using Blind Phase Noise Compensation in the Presence of Jammer Noise**" is a record of my own work carried out towards the partial fulfillment for the award of degree of Master of Engineering in Wireless Communication at Electronics and Communication Engineering Department, Thapar University, Patiala, under the guidance of **Dr. Amit Kumar Kohli**, Associate Professor, Electronics and Communication Engineering Department, Thapar University, Patiala, India during 2016-2017.

The matter presented in this thesis has not been submitted either in part or full to any other university or institute for the award of any other degree.

Date: 14/07/2017

Jasonpreet Kaur

**Jason Preet Kaur**
Roll No. 801563009

It is certified that the above statement made by the student (Ms. Jason Preet Kaur) is correct to the best of my knowledge and belief.

Amit Kohli

14/07/2017

Date:

**Dr. Amit Kumar Kohli**
Associate Professor
ECED, Thapar University
Patiala-147004, (Punjab)

## ACKNOWLEDGEMENT

I would like to express my regards to **Dr. Amit Kumar Kohli, Associate Professor, Electronics and Communication Engineering Department, Thapar University, Patiala, India** for providing me with endless assistance and persistent motivation throughout the research and technical writing. He has provided me profound support in the presentation style of this thesis, and I found his guidance to be worthwhile. Without his support and encouragement in the right direction, this accomplishment would not have been possible.

I am also grateful to the **Dr. Alpana Aggarwal, Head of the Department, Electronics and Communication Engineering Department, Thapar University, Patiala, India** for her encouragement, support and provision of adequate infrastructure for the completion of this thesis.

I would also like to acknowledge the efforts of **Dr. Hem Dutt Joshi, P.G. Coordinator, Electronics and Communication Engineering Department, Thapar University, Patiala, India** for providing necessary information and guidelines during the dissertation report work.

I am also thankful to the entire faculty and staff members of Electronics and Communication Engineering Department, Thapar University, Patiala, India for their selfless and generous assistance.

I am greatly indebted to all my friends, who have graciously applied themselves to the task of helping me with ample morale support and worthy advice whenever I was stuck on a trouble spot. Finally, I would like to extend my gratitude to all those who directly or indirectly provided me uninterrupted aid in pursuing the research work.

**Jason Preet Kaur**

Roll No. 801563009

## ABSTRACT

The popularity of multimedia data services is skyrocketing. The fourth-generation (4G) wireless communication technology is based on orthogonal-frequency-division-multiplexing (OFDM), one of the most reliable multi-carrier technique. It is attributed to its large capacity accommodating more number of users, high data rate and the provision of worldwide coverage with high mobility. Despite this, OFDM is significantly influenced by phase noise due to imperfections of the oscillators. As a result, the presence of phase noise in an OFDM symbol block rotates the constellation and introduces inter-carrier-interference (ICI), which in turn causes loss of orthogonality amid the subcarriers.

The deleterious effects of phase noise can be classified into common-phase-error (CPE) and ICI, and these effects get reflected in the bit-error-rate (BER) performance of the system. It is necessary to compensate for these effects of phase noise, and it is done by the usage of several techniques, which may be pilot-based or blind techniques. The blind compensation techniques are advantageous over the pilot-based techniques because they do not use pilot symbols and as a result, these are bandwidth efficient techniques. One such blind compensation technique has been taken into consideration for the purpose of research in this thesis work.

This research work presents the performance evaluation of a blind algorithm used for compensating the phase noise effects in the wireless OFDM communication systems, in which the time-average of phase noise within an OFDM symbol block is calculated at the subblock level. It contributes towards the estimation of common phase error term, which is used for the excision of ICI. The main focus of presented research work is on the effects of phase noise on the performance of underlying OFDM system for the different number of subcarriers, for the different M-ary phase-shift-keying (PSK) modulation techniques, and it emphasizes on the impact of jammer noise, while using the zero-forcing (ZF) and minimum-mean-square-error (MMSE) techniques for detection. Simulation results are demonstrated to verify efficacy of the blind-phase-noise-compensation (BPNC) technique under the multipath Rayleigh fading environment, which manifest that the MMSE detector performs marginally better than ZF detector in the presence of jammer noise. However, the long OFDM symbol block period or the large number of subcarriers can prove to be helpful in combating the impact of jammer noise.



Keyword - OFDM, Intercarrier Interference, Phase Noise Compensation, Blind Algorithms, M-ary PSK, Jammer Noise.

## TABLE OF CONTENTS

## LISTS OF TABLES

## LISTS OF FIGURES

## LIST OF ACRONYMS

| | |
|---|---|
| **3GPP** | THIRD GENERATION PARTNERSHIP PROJECT |
| **4G** | FOURTH GENERATION |
| **5G** | FIFTH GENERATION |
| **ADSL** | ASYMMETRIC DIGITAL SUBSCRIBER LINE |
| **AWGN** | ADDITIVE WHITE GAUSSIAN NOISE |
| **BER** | BIT ERROR RATE |
| **BPNC** | BLIND PHASE NOISE COMPENSATION |
| **C-MMPSE** | CONSTRAINED MINIMUM MEAN SQUARE PREDICTION ERROR |
| **COFDM** | CODED ORTHOGONAL FREQUENCY DIVISION MULTIPLEXING |
| **CP** | CYCLIC PREFIX |
| **CPE** | COMMON PHASE ERROR |
| **CPEC** | COMMON PHASE ERROR CORRECTION |
| **CSI** | CHANNEL STATE INFORMATION |
| **DAB** | DIGITAL AUDIO BROADCASTING |
| **DFT/FFT** | DISCRETE/FAST FOURIER TRANSFORM |
| **DSL** | DIGITAL SUBSCRIBER LINE |
| **DVB** | DIGITAL VIDEO BROADCASTING |
| **FDM** | FREQUENCY DIVISION MULTIPLEXING |
| **FEC** | FORWARD ERROR CORRECTION |
| **HDSL** | HIGH BIT RATE DIGITAL SUBSCRIBER LINE |
| **HDTV** | HIGH DEFINITION TELEVISION |
| **HIPERLAN** | HIGH PERFORMANCE RADIO LOCAL AREA NETWORK |
| **ICI** | INTERCARRIER INTERFERENCE |

| | |
|---|---|
| **IDFT/IFFT** | INVERSE DISCRETE/FAST FOURIER TRANSFORM |
| **ISI** | INTERSYMBOL INTERFERENCE |
| **LAN** | LOCAL AREA NETWORK |
| **LTE** | LONG TERM EVOLUTION |
| **MCM** | MULTICARRIER MODULATION |
| **ML** | MAXIMUM LIKELIHOOD |
| **MLSD** | MAXIMUM LIKELIHOOD SEQUENCE DETECTION |
| **MMSE** | MINIMUM MEAN SQUARE ERROR |
| **OFDM** | ORTHOGONAL FREQUENCY DIVISION MULTIPLEXING |
| **PAPR** | PEAK TO AVERAGE POWER RATIO |
| **PLL** | PHASE LOCKED LOOP |
| **PN** | PHASE NOISE |
| **PNS** | PHASE NOISE SUPPRESION |
| **PSK** | PHASE SHIFT KEYING |
| **RF** | RADIO FREQUENCY |
| **RV** | RANDOM VARIABLE |
| **SNR** | SIGNAL TO NOISE RATIO |
| **VoIP** | VOICE OVER INTERNET PROTOCOL |
| **VSDL** | VERY HIGH BIT RATE DIGITAL SUBSCRIBER LINE |

# CHAPTER-1
# INTRODUCTION

**C**onnectivity is one of the major requirements for survival. Irrespective of when and where, a user should always be able to communicate. The invention of wireless telegraphy (a radio transmission technique that required no wires) by Marconi in 1899 was a major breakthrough in the industry of wireless communication [1]. This motivated the researchers to work in the field of communication, hence paving the way for an era of wireless mobile communication; advanced yet affordable, in contrast to the wired communication. Over the years, the number of users indulging in the wireless communication has increased, and so have the demand for high-data-rate services. These services, comprising of the exchange of information over Internet, voice-over-Internet-protocol (VoIP), multimedia and live video streaming, have opened newer dimensions for the future communication systems. In order to fulfil the need of increasing number of users, it is necessary to utilize the available spectrum in an effective manner. This can be achieved by the use of bandwidth efficient modulation techniques. In addition to efficient usage of spectrum, these techniques should be robust to the multipath propagation over the wireless channel. Such schemes are referred to as the multi-carrier-modulation (MCM) techniques. In contrast to single-carrier (SC) systems, where a single carrier occupies the entire bandwidth, the MCM techniques are more reliable and provide high data rates. These allow numerous users to transmit as well as receive data in an allotted band by splitting the entire available bandwidth into many narrowband subcarriers. The multiple carriers are chosen such that they are orthogonal to each other, accordingly reducing the spacing between them. These striking features encourage us to study orthogonal-frequency-division-multiplexing (OFDM) [2], an MCM technique, which differs from the frequency-division-multiplexing (FDM) [3] only in terms of the orthogonality of carriers.

It is noteworthy that the MCM technique is a viable approach capable of providing high data rates under high user mobility scenario as well. In SC systems, one data symbol is sent over a single carrier. However, in OFDM that makes use of MCM, $N$ complex data symbols (i.e., M-PSK) are transmitted in parallel rather than a serial transmission, after modulating them over $N$ orthogonal subcarriers. The orthogonality of carriers alleviates the spacing between channels. Each carrier in OFDM is modulated over the low data rate stream. However, the effective data rate in SC and OFDM remains consistent. Moreover, the time period of the system to process signal with parallel transmissions increases.

The terrestrial radio channel is known for its time-dispersive nature. It is a distortion encountered in the time-domain that gives rise to spreading of modulated symbols. The

spreading results in overlapping of consecutive symbols eventually resulting in the interference among them, in other words, inter-symbol-interference (ISI). Delay spread is responsible for the frequency-selective nature of the channel, when it is larger than the symbol period. Since the characteristics of multipath fading are not predictable for the frequency-selective channels, it is hard to compensate it. However, the usage of MCM technique has proved to be helpful in resolving this issue by increasing the symbol duration. Another critical problem is inter-carrier-interference (ICI) because of the violation of orthogonality, which arises when the OFDM symbol passes through a time-dispersive channel. A cyclic-prefix (CP) has been a near to perfect solution in preserving orthogonality. It is appended in the beginning of every OFDM symbol, providing periodicity to the OFDM symbol block [4]. This periodicity is maintained by using inverse-discrete-Fourier-transform (IDFT). Hence, use of CP removes both ISI and ICI problems altogether.

## 1.1 EVOLUTION OF OFDM

Although OFDM based systems have become popular only recently, but their usage dates back to the period of Second World War, when US military forces used it in high frequency systems e.g., KINEPLEX, ANDEFT, and KATHRYN etc. Chang proposed first promising development in the multicarrier system design in 1966. He obtained his first OFDM patent in 1970 for presenting a theoretical approach for the parallel transmission of data through a linear band limited channel [5]. In 1971, Weinstein *et al.*, proposed usage of discrete-Fourier-transform (DFT) for the baseband modulation and demodulation. This proved to be a major advancement in OFDM communication systems. Until this time, the guard period was used in frequency domain in order to mitigate ISI as well as ICI. Peled and Ruiz introduced cyclic prefix in 1980, which was another turning point in OFDM evolution history as it settled the issue of maintaining orthogonality of subcarriers [6]. Due to the availability of low cost processors for DFT operations (fast-Fourier-transform (FFT)) and use of CP, the OFDM became an integral part of telecommunication industry. Wideband data communication over the radio channels benefitted from OFDM in 1990s. OFDM has been extensively used in *x*-digital-subscriber-line (*x*DSL). Commercially, OFDM technology has been used in digital-audio-broadcasting (DAB) [7] and digital-video-broadcasting (DVB) [8] with high-definition-television (HDTV) terrestrial broadcasting standard. Wireless local area networks have also adopted OFDM at physical layer e.g., in high-performance-radio-local-area-network (HIPERLAN/2) and IEEE 802.11a.

It has been successfully employed in the third-generation-partnership-project (3GPP), 3GPP2 and long-term-evolution (LTE). Perhaps because of exclusive striking features, it has become a preferable technique to be used in the next generation fourth-generation (4G) systems. Despite the reliable and robust nature of OFDM systems, these are highly sensitive to the oscillator imperfections, which appear in the form of phase noise at the receiver side. Analysing today's scenario, the phase noise has become a critical issue, and hence it is imperative to limit the levels of phase noise; otherwise the system may lose its credibility. And this is achieved via certain algorithms and techniques that compensate the adverse effect of phase noise.

The future of mobile communication, fifth-generation (5G) technology is already under research procedure, and it has been recognized that in the upcoming years, the current technologies will fail to meet the exponentially increasing requirement of high spectral efficiency along with exorbitant data rates; therefore, the research campaign for exploring suitable technologies has already begun.

Figure 1.1 comprehensively depicts the advancements in the field of wireless communication technology over the years in chronological order.

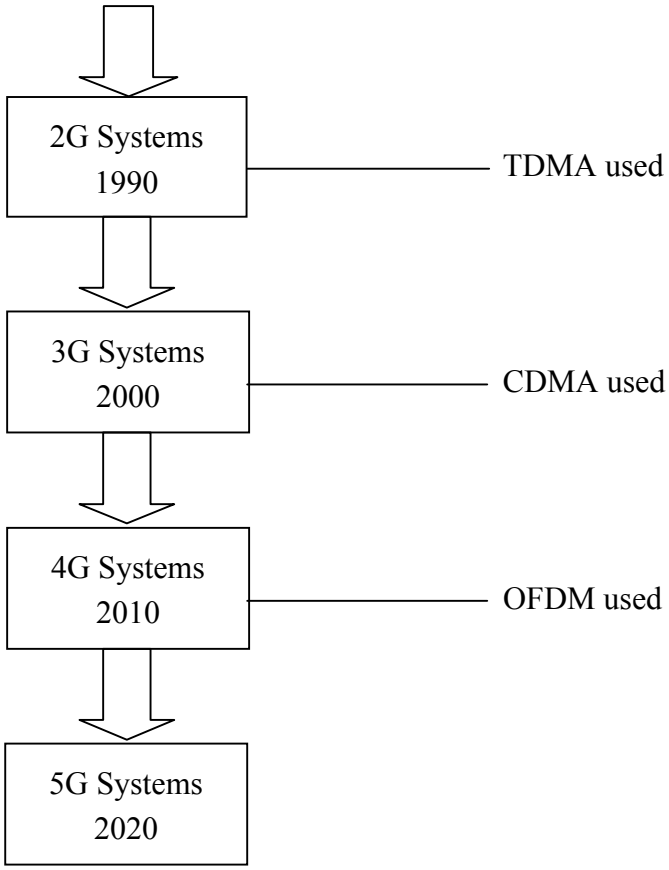


Figure 1.1 A flowchart depicting the advancements in wireless communication technologies

## 1.2 OFDM TRANSCEIVER SYSTEMS

Figure 1.2 describes an OFDM transceiver system, which excludes forward-error-correction (FEC) code and interleaving blocks. These two blocks are a part of coded-OFDM (COFDM) system in order to make the system robust against burst errors.

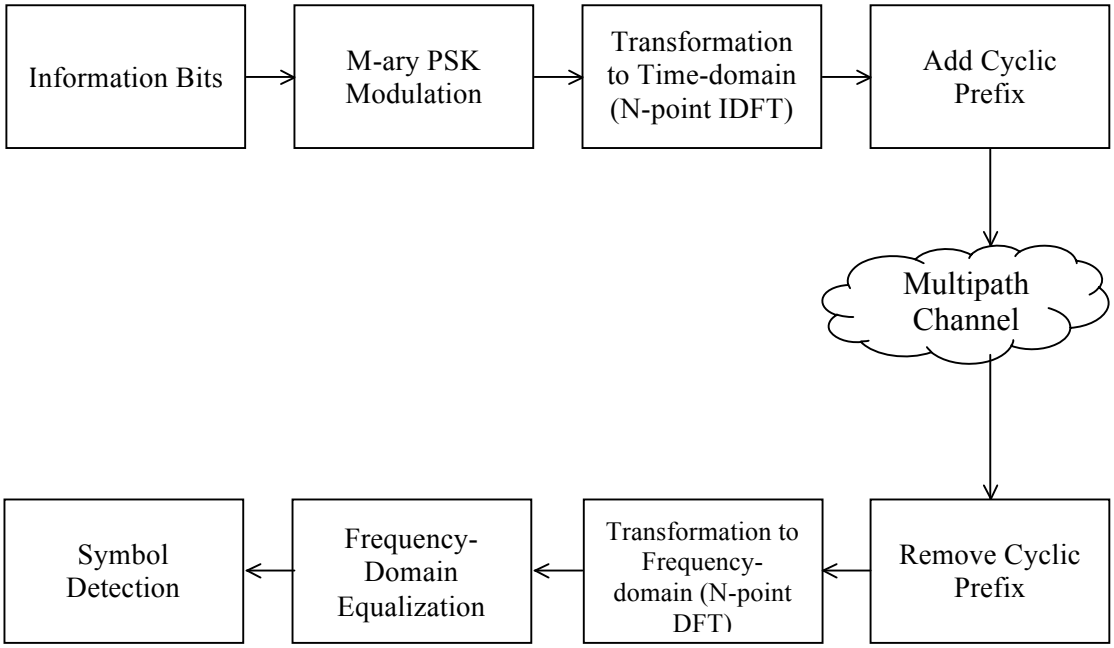


Figure 1.2 Basic OFDM system model with no anomalies
(i.e. without additive-white-Gaussian-noise (AWGN) and/or jammer noise)

The binary input data are assembled in the form of groups (e.g., 1-bit for BPSK, 2-bit group for QPSK, 3-bit group for 8-PSK, 4-bit group for 16-PSK etc.), and consequently mapped onto corresponding constellation points. The serial bit stream consists of complex data, which is transformed into the parallel stream of data using a serial to parallel converter. The resulting parallel bit stream is input to IDFT block. Depending on the number of subcarriers say $N$, the parallel data is grouped into a block of $N$ data symbols. One of the captivating features of OFDM is cyclic prefix, which is used to provide robustness against channel multipath and combat ISI. It is prepended to every OFDM block of $N$ data symbols, and then the obtained OFDM signal is ready to be transmitted though a time-dispersive multipath-fading channel [9], [10]. The OFDM symbol is transmitted under the Rayleigh multipath fading conditions [11], [12]. The OFDM signal propagates through a wireless channel (which is prone to anomalies) and therefore, the received signal is a modified version of the transmitted signal. The most critical of all issues associated with OFDM is the presence of phase noise in the received OFDM signal, which is defined as the phase alteration in OFDM symbol that occurs due to a mismatch in the carrier frequency of transmitter and receiver

oscillators [13]. The phase noise affects the OFDM signal and it is hence necessary to nullify its effects by employing proper algorithms and techniques. The received signal is then demodulated using DFT, and de-mapped in accordance with the transmitter constellation specifications. As a result, the output data stream is recovered.

## 1.3 BENEFITS OF OFDM SYSTEM

OFDM technology possesses many remarkable features, which have made it a technology of choice in the 4G wireless communication systems. Some of these are described below

### 1.3.1 Combating ISI and Mitigating ICI

The orthogonality of the subcarriers can be jeopardized when the OFDM signal passes through the multipath channel. Use of cyclic prefix maintains the orthogonality of the subcarriers [4]. Before cyclic prefix, a guard interval was used for the purpose. It is defined as the unused space between any two OFDM symbols. This vacant space behaved like a buffer for multipath reflection. But in practice, the empty interval introduces a crosstalk between different subcarriers known as ICI; as a result, the subcarriers are no longer orthogonal to each other. To overcome this problem, a replica of the end portion of OFDM symbol block of a certain-defined length is appended in front of the transmitted OFDM symbol block. This is known as cyclic prefix, and it has the same time interval as the guard interval. However, it makes sure that the delayed copies of an OFDM symbol have whole symbol block within DFT window; hence we observe that the transmitted symbol is periodic. So, CP removes the effect of ISI by occupying the empty guard period and mitigates ICI by retaining the orthogonality of subcarriers.

### 1.3.2 Spectral Efficiency

OFDM is preferably used over FDM systems because it is more bandwidth efficient. In FDM, the subcarriers are spaced apart without any overlapping. While, in the case of OFDM, due to the orthogonal feature, the subcarriers overlap each other. As a result, the bandwidth used is reduced immensely, making OFDM spectrally efficient technique.

1.3.2.1 *Principle of Orthogonality*

As we know, had the FDM system been able to implement an orthogonal set of subcarriers, the spectral efficiency would have been improved. The orthogonality of the subcarriers ensures overlapping of the subcarriers without any interference from other distinct subcarriers. Undeterred by the overlapping subcarriers, the individual subcarrier signal can be obtained, if an only if orthogonality is maintained.

Any two signals are declared orthogonal, if the dot product of such signals is zero. Any two uncorrelated stochastic processes are orthogonal. We know that the DFT of sinusoids manifest as the orthogonal basis group. Any signal may be expressed as linear grouping of these orthogonal sinusoidal signals in the vector space of DFT. Therefore, DFT is utilized at transmitting point of OFDM to place the desired data bits onto the orthogonal subcarriers. Similarly, at the receiver side, IDFT is used to recover the data bits by processing the subcarriers.

The principle of orthogonality can be implemented in OFDM in order to minimize the usage of bandwidth. As the aim specifies, the purpose can be achieved by reducing the spacing between the subcarriers, which in turn can only be obtained by the use of orthogonality principle.

Analytically, any two time-domain continuous signals $g_1(t)$ and $g_2(t)$ are said to be orthogonal, over the time interval $[t, t+T]$, where $T$ is the time period, if

$$\frac{1}{T}\int_{t}^{t+T} g_m(t) \times g_n(t)\, dt = 0 \qquad if\ m \neq n \tag{1.1}$$

In OFDM, the subcarriers are represented as $g_m(t) = e^{j2\pi g_m t} = e^{\frac{j2\pi mt}{T}}$ and therefore, the principle of orthogonality for OFDM systems may be represented as

$$\frac{1}{T}\int_{0}^{T} e^{j2\pi g_m t} \times e^{-j2\pi g_n t}\, dt = 0 \qquad \forall\ m \neq n \tag{1.2}$$

If the value of integral is 1, the signals will be orthonormal.

For discrete-time signals with sampling interval at $t = kT_s = kT/N$, $k = 0,1,...,N-1$, the principle of orthogonality can be expressed as

$$\frac{1}{T}\sum_{n=0}^{N-1} e^{\frac{j2\pi m}{T}kT_s} \times e^{-\frac{j2\pi n}{T}kT_s} = \frac{1}{T}\sum_{n=0}^{N-1} e^{\frac{j2\pi(m-n)}{N}k} = 0 \qquad \forall\ m \neq n \tag{1.3}$$

So, the OFDM based communication systems effectively use the available spectrum through the overlapping of orthogonal subcarriers. The overlapping subcarriers are completely different from each other because, maximum power location of a subcarrier in frequency-domain corresponds with the minimum power location of the adjacent subcarriers; hence, avoiding any kind of interference.

### 1.3.3 Ease of Implementation

The MCM techniques involve multiple subcarriers, which may pose a problem in implementation, because a bank of modulators/demodulators may be needed for the same. But, OFDM rules out any such problem because it uses IFFT/FFT for the purpose of modulation/demodulation at transmitting/receiving end respectively. This eases procedure for the implementation of the principle of OFDM.

### 1.3.4 Equalization

In SC systems, frequency-selective channel gets transformed into flat faded channel because of equalization; however, it also amplifies the noise component present in the signal. This affects the performance of the SC systems due to higher attenuation at some frequencies than others. Instead in orthogonal frequency division multiplexing, wideband frequency-selective channel is interpreted as a group of narrowband flat fading sub-channels, and this reduces the extent of complexity of equalization at the receiver side.

## 1.4 OFDM SYSTEM WORKING UNDER DISPERSIVE ENVIRONMENT

A traditional OFDM has been demonstrated in Figure 1.2. The complex frequency-domain input data to the IDFT (or IFFT) block is $\vec{X} = \left[\bar{X}_0, \bar{X}_1, ..., \bar{X}_{\bar{N}-1}\right]^T$, where $\bar{N}$ denotes the number of subcarriers; and each element of the complex vector $\vec{X}$ i.e., $\bar{X}_k$ represents a specific constellation point in accordance with the modulation scheme. This frequency-domain data is transformed into time-domain by utilizing IDFT (or IFFT) operation, and

hence, we obtain $\vec{x} = \left[\bar{x}_0, \bar{x}_1, ..., \bar{x}_{\bar{N}-1}\right]^T$, where each element of the time-domain data vector can be represented as [14],

$$\bar{x}(n) = \frac{1}{\sqrt{\bar{N}}} \sum_{k=0}^{\bar{N}-1} \bar{X}(k) \exp\left(j \frac{2\pi kn}{\bar{N}}\right), \qquad 0 \le n \le \bar{N}-1 \tag{1.4}$$

When this OFDM signal passes through a wireless channel, additive-white-Gaussian-noise (AWGN) is added to this signal, and therefore, the received OFDM signal in time-domain can be expressed as

$$\bar{y}(n) = \bar{x}(n) + \bar{w}(n), \qquad 0 \le n \le \bar{N}-1 \tag{1.5}$$

where, $\bar{w}(n)$ represents the AWGN samples with zero-mean and variance $\sigma_{\bar{w}}^2$. The received time-domain OFDM signal is transformed into the frequency-domain signal by using DFT (or FFT), and the resultant signal can be expressed as

$$\bar{Y}(k) = \frac{1}{\sqrt{\bar{N}}} \sum_{n=0}^{\bar{N}-1} \bar{y}(n) \exp\left(-j \frac{2\pi kn}{\bar{N}}\right), \qquad 0 \le k \le \bar{N}-1 \tag{1.6}$$

$$= \bar{X}(k) + \bar{W}(k), \qquad 0 \le k \le \bar{N}-1 \tag{1.7}$$

where, $\bar{Y}(k)$, $\bar{X}(k)$ and $\bar{W}(k)$ represent the $\bar{N}$-point DFT (or FFT) normalized coefficients of $\bar{y}(n)$, $\bar{x}(n)$ and $\bar{w}(n)$ respectively. $\bar{X}(k)$ and $\bar{W}(k)$ are given as

$$\bar{X}(k) = \frac{1}{\sqrt{\bar{N}}} \sum_{n=0}^{\bar{N}-1} \bar{x}(n) \exp\left(-j \frac{2\pi kn}{\bar{N}}\right), \qquad 0 \le k \le \bar{N}-1 \tag{1.8}$$

$$\bar{W}(k) = \frac{1}{\sqrt{\bar{N}}} \sum_{n=0}^{\bar{N}-1} \bar{w}(n) \exp\left(-j \frac{2\pi kn}{\bar{N}}\right), \qquad 0 \le k \le \bar{N}-1 \tag{1.9}$$

Orthogonal subcarriers are one of the salient features of OFDM wireless communication systems, but the orthogonality is jeopardized when the OFDM symbol block propagates through a time-dispersive wireless channel. As a result, ICI and ISI are introduced. To eliminate these adverse effects, a cyclic-prefix (CP) is utilized. The cyclic prefix is a replica

of the end portion of OFDM symbol block, and it is appended to the beginning of the respective OFDM symbol block, as illustrated in Figure 1.3. The cyclic prefix length is $\bar{N}_C$.

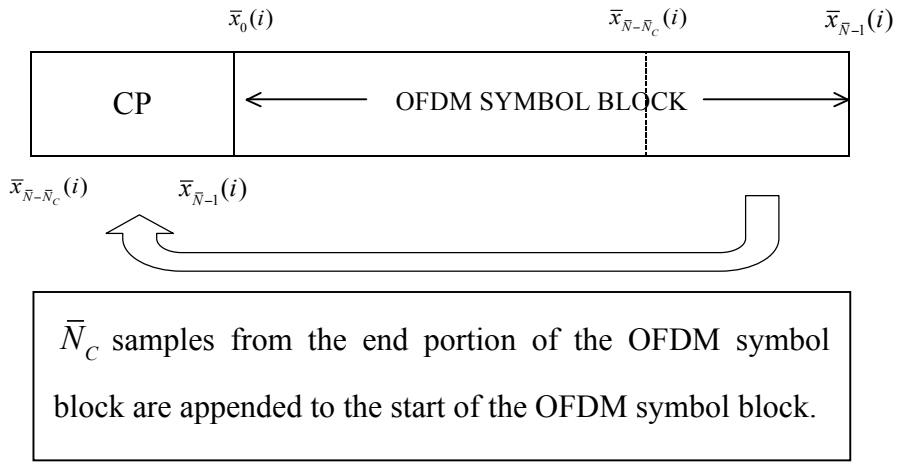


Figure 1.3 Time-domain OFDM symbol block at time instant *i* using cyclic prefix

Therefore, the actual OFDM symbol block transmitted over a wireless channel at time instant *i*, is $\vec{x}_T(i) = \left[\bar{x}_{\bar{N}-\bar{N}_C}(i),...,\bar{x}_{\bar{N}-1}(i),\bar{x}_0(i),\bar{x}_1(i),...,\bar{x}_{\bar{N}-1}(i)\right]^T$. When CP is used, any distortion that arises due to linear dispersive channel can be rectified by utilizing one-tap equalizer. In order to, understand the role of one-tap equalization, let us assume that the received time-domain OFDM signal is a linear combination of different versions of transmitted OFDM signal, each having different delay as well as gain. i.e.,

$$\bar{y}(\bar{t}) = \bar{g}_1\bar{x}(\bar{t}+\bar{\tau}_1) + \bar{g}_2\bar{x}(\bar{t}+\bar{\tau}_2), \tag{1.10}$$

The usage of CP eliminates ICI as well as ISI, subject to the conditions that the delay spread i.e., $\bar{\tau}_2 - \bar{\tau}_1$ is less than $\bar{N}_C$; and the DFT (or FFT) window at the receiving end is perfectly aligned with OFDM symbol block period of first symbol block. Mathematically, the effect of dispersive channel on the received OFDM symbol block (continuous-times) on *k*th subcarrier ($0 \le k \le \bar{N}-1$) can be interpreted as

$$\bar{y}\left(k,\bar{t}\right)=\frac{1}{\sqrt{\bar{N}}}\bar{g}_1\bar{X}\left(k\right)\exp\left(j\frac{2\pi k\left(\bar{t}-\bar{\tau}_1\right)}{\bar{T}}\right)+\frac{1}{\sqrt{\bar{N}}}\bar{g}_2\bar{X}\left(k\right)\exp\left(j\frac{2\pi k\left(\bar{t}-\bar{\tau}_2\right)}{\bar{T}}\right), \tag{1.11}$$

where, $\bar{T}$ is the OFDM symbol block period. In order to align the DFT (or FFT) window with the start of first OFDM symbol block, it must be offset by a factor of $\bar{\tau}_1$,

$$\bar{y}\left(k,\bar{t}\right)=\frac{1}{\sqrt{\bar{N}}}\bar{g}_1\bar{X}\left(k\right)\exp\left(j\frac{2\pi k\bar{t}}{\bar{T}}\right)+\frac{1}{\sqrt{\bar{N}}}\bar{g}_2\bar{X}\left(k\right)\exp\left(j\frac{2\pi k\left(\bar{t}-(\bar{\tau}_2-\bar{\tau}_1)\right)}{\bar{T}}\right), \tag{1.12}$$

$$\bar{y}\left(k,\bar{t}\right)=\frac{1}{\sqrt{\bar{N}}}\bar{X}\left(k\right)\exp\left(j\frac{2\pi k\bar{t}}{\bar{T}}\right)\times\left(\bar{g}_1+\bar{g}_2\exp\left(-j\frac{2\pi k\left(\bar{\tau}_2-\bar{\tau}_1\right)}{\bar{T}}\right)\right), \tag{1.13}$$

Performing demodulation and $\bar{N}$-point DFT (or FFT) operation on the received continuous time-domain OFDM signal $\bar{y}\left(k,\bar{t}\right)$ in the presence of noise, we obtain

$$\bar{Y}\left(k\right)=\bar{X}\left(k\right)\left(\bar{g}_1+\bar{g}_2\exp\left(-j\frac{2\pi k\left(\bar{\tau}_2-\bar{\tau}_1\right)}{\bar{T}}\right)\right)+\bar{W}\left(k\right), \tag{1.14}$$

$$=\bar{H}\left(k\right)\bar{X}\left(k\right)+\bar{W}\left(k\right),\qquad 0\le k\le\bar{N}-1 \tag{1.15}$$

where, $\bar{H}\left(k\right)$ denotes the dispersive channel tap-coefficients, and it can be denoted using Equation (1.14) as

$$\bar{H}\left(k\right)=\bar{g}_1+\bar{g}_2\exp\left(-j\frac{2\pi k\left(\bar{\tau}_2-\bar{\tau}_1\right)}{\bar{T}}\right), \tag{1.16}$$

Equation (1.15) exhibits that in frequency-domain, the received OFDM signal is a multiplication of transmitted OFDM signal as well as respective channel gain coefficient i.e., $\bar{X}\left(k\right)$ and $\bar{H}\left(k\right)$; therefore, the estimate of transmitted data i.e., $\hat{\bar{X}}\left(k\right)$ can be obtained by applying one-tap equalizer principle. It follows that

$$\hat{\bar{X}}\left(k\right)=\frac{\bar{Y}\left(k\right)}{\bar{H}\left(k\right)}, \tag{1.17}$$

$$= \bar{X}(k) + \frac{\bar{W}(k)}{\bar{H}(k)}, \qquad 0 \le k \le \bar{N} - 1 \tag{1.18}$$

However, this procedure may lead to noise enhancement when $\bar{H}(k)$ is small.

## 1.5 DRAWBACKS OF OFDM SYSTEM

We have seen that OFDM has many striking features, but it has many disadvantages, out of which the most critical are high peak-to-average-power-ratio; timing and frequency susceptibility at the receiver.

### 1.5.1 High Peak-to-Average-Power-Ratio (PAPR)

In comparison to SC systems, OFDM systems are known to have more PAPR because in OFDM systems, many subcarrier components are added in the time-domain as a result of IDFT operation. High PAPR degrades the signal-to-quantization-noise ratio, which in turn reduces efficiency factor for power amplifier [14]. Hence, it is important to take measures to reduce the PAPR up to permissible levels.

### 1.5.2 Phase Noise and Frequency Offset

One of the most highlighting limitations of OFDM systems is that these systems show high sensitivity to phase noise. The phase noise arises as a result of local oscillators, which show imperfections in practical usage. The difference between the phase of carrier signal and the phase of local oscillating equipment is called the phase noise [13], [14]. This sensitivity issue causes an uncompromising constraint on fabrication of the circuit as well as oscillators to be used in the designing process. It is therefore essential to compensate for the effects of phase noise by use of efficient and suitable algorithms.

## 1.6 APPLICATIONS OF OFDM

In recent years, OFDM modulation technique has moved out of treatise into the world of implementation, where it is used in numerous applications. These techniques are used in data delivery over conventional phone lines, wireless networks and digital broadcasting services. Some of these are briefly described in the Table 1.1. In addition to these, OFDM can also be

used in applications involving optical systems. However, the implementation of OFDM in the later years in the field of optical communication may depend on the advantages, disadvantages and cost of implementation associated with the process. But, it intends to deliver high-speed services.

| OFDM Applications | Attributes | Data Rate |
|---|---|---|
| Digital Subscriber Lines (*x*DSL) | Uses broadband modem to provide high-speed internet service.<br>• HDSL: Requires two separate lines from normal phone line. It downloads and uploads at same rate.<br>• ADSL: Uses spectrum available on regular phone lines, which is not utilized for voice calls. Download speed is higher than upload speed. It is predominantly used for residential users.<br>• VDSL: It works over shorter distances and uses standard phone wiring. It is asymmetric just like ADSL. | 1.5 - 2 Mbps<br>Downstream: 1.5 – 6.1 Mbps<br>Upstream: 16-640 Mbps<br>Downstream: 25 – 55 Mbps<br>Upstream: 3.2 Mbps |
| Digital-audio-broadcasting (DAB) [7] | • It is a European standard that uses DQPSK modulation scheme particularly used for the transmission of text, images and sounds.<br>• It is a wideband broadcasting technique expected to replace the existing analog modulation techniques AM and FM etc.<br>• Band III and L-band have been allocated for it and it has four transmission modes (I, II, III, IV).<br>• Robust against noise and multipath fading in mobile communication. | 1.2 Mbps |
| Digital-video-broadcasting (DVB) [8] | • An ETSI standard used for transmission of high definition pictures and audio over satellites, cables and mobile vehicles.<br>• It makes use of QPSK and QAM modulation techniques, and it is widely used in<br>➢ DVB-terrestrial<br>➢ DVB-satellite<br>➢ DVB-handheld<br>➢ Integrated services digital broadcasting standards | As high as 31 Mbps |

Table 1.1 Applications of OFDM in Wireless Communication Systems (cont…..)

| OFDM Applications | Attributes | Data Rate |
|---|---|---|
| IEEE 802.11 [15] | • Specification of media-access (MAC) and physical (PHY) layer are combined in order to implement wireless-local-area-networking (WLANs).<br>• This workgroup comprises of half duplex wireless means of communication over 900 MHz, 2.4 GHz, 3.5 GHz, 5 GHz and 60 GHz frequency bands.<br>➢ 802.11a was released in 1999. It uses OFDM and operates in 5-3.7 GHz frequency band.<br>➢ 802.11b, a widely accepted standard was released in later 1999 operating in 2.4 GHz band but it utilizes direct-sequence-spread-spectrum (DSSS).<br>➢ 802.11g was established in 2003, which operates in 2.4 GHz band and uses OFDM just like 802.11a<br>➢ 802.11n, an improvement to previous standards. It utilizes multiple-input-multiple-output (MIMO) antennas and operates in both 2.4 and 5 GHz bands. | 1.5 – 54 Mbps<br>11 Mbps<br>54 Mbps<br>54 – 600 Mbps |
| IEEE 802.16e | • WiMAX (interoperable implementation of IEEE 802.16 set of standards) has added support for mobility over long range.<br>• Spectrum profiles include 2.3 GHz, 2.5 GHz and 3.5 GHz band.<br>• Low-cost implementation and use of MIMO technology make it economically viable standard. | 15-70 Mbps |
| HIPERLAN/2 (High-performance-radio-local-area-network) | • Developed by ETSI to achieve high data as compared to IEEE 802.11 standard.<br>• It is a connection-oriented technology that uses OFDM.<br>• It operates in 5 GHz band. | 54 Mbps |

Table 1.1 Applications of OFDM in Wireless Communication Systems

## 1.7 MATHEMATICAL UNDERSTANDING OF ADVERSE PHASE NOISE EFFECTS UNDER IDEAL CHANNEL CONDITIONS

An OFDM symbol block propagates through a wireless channel. This wireless channel is known to be imperfect in practical situation, and introduces distortion in the OFDM signal. Before considering multipath channel, let us consider a case, where the channel is ideal as discussed by Armstrong in [14]. This implies that there is no AWGN component introduced in the signal when it passes through a wireless channel, no amplitude attenuation, and no distortion or noise of any kind.

Mathematically, it can be represented as $\hat{W}[k] \to 0$, where $\hat{W}[k]$ represents the additive noise component; and the frequency-domain channel gain $\hat{H}[k]$ is assumed to be ideal i.e., unity. When an OFDM symbol propagates through such a channel, the received time-domain signal samples can be expressed as

$$\hat{r}[n] = \hat{g}[n]\exp\left(j\hat{\phi}[n]\right), \qquad 0 \le n \le \hat{N}-1 \tag{1.19}$$

where, $\hat{\phi}[n]$ is the phase noise for $n$th subcarrier, $\hat{g}[n]$ is the transmitted OFDM signal sample and $\hat{N}$ is the number of subcarriers.

If the phase error is considered to be constant i.e., $\hat{\phi}[n] = \hat{\phi}_0$, then it can be simplified as

$$\hat{r}[n] = \hat{g}[n]\exp(\hat{\phi}_0), \tag{1.20}$$

Taking $\hat{N}$-point DFT, the frequency-domain signal can be expressed as

$$\hat{R}[k] = \exp(\hat{\phi}_0)\hat{G}[k], \qquad 0 \le k \le \hat{N}-1 \tag{1.21}$$

This indicates that the constellation is rotated by an angle $\hat{\phi}_0$.

However, if the phase noise is a zero-mean process and any two phase noise samples are uncorrelated i.e., $E[\hat{\phi}[n]\hat{\phi}[m]] = 0,\ n \ne m$, where $E[.]$ indicates the expectation operation. After taking normalized $\hat{N}$-point DFT, we obtain

$$\hat{R}[k] = \frac{1}{\sqrt{\hat{N}}}\sum_{n=0}^{\hat{N}-1}\hat{r}[n]\exp\left(-j\frac{2\pi kn}{\hat{N}}\right)$$
$$= \frac{1}{\sqrt{\hat{N}}}\sum_{n=0}^{\hat{N}-1}\hat{g}[n]\exp\left(j\hat{\phi}[n]\right)\exp\left(-j\frac{2\pi kn}{\hat{N}}\right), \qquad 0 \le k \le \hat{N}-1 \tag{1.22}$$

For smaller values of phase noise, it can be approximated by using Taylor series expansion $\exp\left(j\hat{\phi}[n]\right) \approx 1 + j\hat{\phi}[n]$, and therefore, the frequency-domain received signal can be represented as

$$\hat{R}[k] \approx \frac{1}{\sqrt{\hat{N}}}\sum_{n=0}^{\hat{N}-1}\hat{g}[n]\left(1 + j\hat{\phi}[n]\right)\exp\left(-j\frac{2\pi kn}{\hat{N}}\right),$$

$$= \hat{G}[k] + \frac{1}{\sqrt{\hat{N}}}\sum_{n=0}^{\hat{N}-1}j\hat{\phi}[n]\hat{g}[n]\exp\left(-j\frac{2\pi kn}{\hat{N}}\right),$$

$$= \hat{G}[k] + P\hat{H}[k], \qquad 0 \le k \le \hat{N}-1 \tag{1.23}$$

where, $P\hat{H}[k]$ denotes the noise term depending on the transmitted OFDM symbol block, and it is a combination of ICI as well as rotated constellation.

However, the situation becomes cumbersome when the same OFDM signals encounter frequency-selective fading while working over wireless channels. We will have to switch to advance statistical techniques for the detection of OFDM information symbols. Unfortunately, if AWGN and/or jammer noise comes into picture, the transmission of OFDM signals gets contaminated. Under this scenario, we need efficient phase noise compensation techniques, noise suppression schemes and compliant demodulation methods. But for all these, we require to do BER performance evaluation of the intended OFDM system used for the data transmission.

## 1.8 PROBLEM STATEMENT

The performance of system can be enhanced by suppressing and compensating the phase noise. Various techniques have been suggested to eliminate adverse effects of phase noise [27]-[38]. The blind techniques for phase noise compensation are known to improve bandwidth efficiency, as they do not utilize pilot symbols [36], [37], [38]. Lee et al., [38] have reported a blind procedure for phase noise compensation, in which single OFDM

symbol block is segregated into subblocks, to approximate the time-average of phase noise over every subblock. This time-averaged phase noise and N-point DFT possess an important relation with the OFDM symbol and channel gain [38]. Based on this relation, the estimated phase noise in this single OFDM symbol block duration is used to compensate for the CPE along with the ICI mitigation. However under deleterious conditions, the jammer noise may be present to adversely affect the BER performance of the underlying orthogonal frequency division multiplexing system, in combination with additive-white-Gaussian-noise (AWGN).

In this thesis, we focus on the influence of jammer noise on the capability of blind-phase-noise-compensation (BPNC) technique for OFDM systems (as proposed by Lee *et al.*, in [38]). The concept of noise bucket effect eventually comes into picture, while dealing with jammer noise, in which the jammer noise is considered to be spread out over N number of subcarriers at the receiver during DFT operation [39]. This spreading effect characterizes the jammer noise as Gaussian at the output irrespective of the noise distribution at the receiver input [40]. Therefore, the presented research work includes the performance evaluation of orthogonal frequency division multiplexing techniques using BPNC, while facing interruption due to jammer noise (exhibiting different statistical parameters), at different number of subcarriers and using different M-ary PSK constant modulation techniques under the multipath Rayleigh fading conditions.

## 1.9 OUTLINE OF THE THESIS

This dissertation contains the analysis of phase noise problem inherent to the OFDM system due to circuit ambiguities, which is encountered during the performance evaluation of underlying system in the presence of phase noise. Subsequently, the performance evaluation of a BPNC technique is presented. The thesis is organized as follows

Chapter 2 elaborates a detailed literature survey done to analyse the phase noise effects and different phase noise compensation techniques used in the OFDM system. Initially, the introduction to phase noise is discussed, which is followed by the phase noise modelling and the influence of phase noise on the orthogonal frequency division multiplexing systems. Different techniques for compensation of phase noise are described i.e., both pilot-based techniques and blind compensation techniques, like phase noise suppression algorithm, iterative procedures depending on subblock processing and blind compensation for phase noise algorithm. Finally, the literature review of BPNC is presented.

Chapter 3 describes the system model of an OFDM system, which is impaired by the jammer noise. The transmitter, channel model and the receiving end of such a system is

described in detail in order to analyse the nature of influence of phase noise as well as jammer noise on orthogonal frequency division multiplexing technique. The characteristics/features of BPNC technique are evaluated for the different number of subcarriers, for the different M-ary PSK digital modulation techniques and the level of jammer noise. These performance evaluations are conducted by using statistically independent MatLab simulation trials.

At last, the concluding remarks are given in chapter 4 along with the possibilities for future research work in the direction of improving BER performance.

# CHAPTER -2
# LITERATURE REVIEW

---

*This chapter encapsulates the literature that has been proposed and recorded in the past, in context of phase noise present in the OFDM systems. Various practically used models of phase noise are also discussed. Particularly, the discussion revolves around the impact of phase noise on OFDM systems under the influence of jammer noise. The performance of such an impaired OFDM system is expected to degrade. So, it is necessary to rectify the degradation to some extent, and this can be pursued by the use of phase noise compensation techniques. Such methods have been examined in this chapter in a nutshell. Typically, the performance of an OFDM system is analyzed with regard to the bit error rate.*

---

## 2.1 TIME-DISPERSIVE CHANNEL

To convey data or information from a transmitter to receiver, a medium is required and this medium can be characterized as a physical link e.g., wire or logical link e.g., radio-frequency (RF) channel [10]. Based on the type of medium, the channel can be classified as guided or unguided. A guided channel exists in the form of a physical connection between sender and receiver, and these physical connections can be in the form of

- Wire (copper wires or twisted pairs)
- Fibre (optical fibre)
- Co-axial cable
- Microwave guides

However, an unguided channel is characterized as the logical association of the transmitter and receiver, and it can be present in the form of

- Acoustic channel
- Wireless channel

A signal transmitted through a wireless channel is susceptible to various impediments. These factors can influence various signals differently depending upon the environmental and geographical conditions, topology etc.

Any signal gets attenuated when it passes over a wireless multipath channel [16]. Also, additive-white-Gaussian-noise (AWGN) influences the signal. The variation in the signal is represented analytically by the convolution operation; and AWGN appears as an extra additive component. A wireless channel is often characterized by the presence of mobile terminals along with fixed terminals. Due to mobility, the channel undergoes dispersion in time-domain and frequency-domain. In this research work, we have considered the time-dispersion as the dominant impediment. We already know that the multipath propagation causes the transmitted beam to get reflected, scattered or diffracted. Moreover, the mobility of the terminals is responsible for non-existence of the direct line-of-sight path between the end terminals. So, the multiple signals arrive at the receiving end with certain delay. As a result, time-dispersion of the signal occurs.

The fluctuations in received signal strength manifests fading. Fading in wireless communication is classified as small-scale and large-scale fading. Amplitude fluctuations and multipath delays in the received signal are the predominant causes of the small-scale fading. The multiple replicas of same signal arriving at the receiving end involve some amount of delay. The time involved in intercepting the first copy and last copy of the signal is termed as the delay spread. A signal propagating through such multipath channel undergoes changes due to various phenomena like

- Reflection (Occurs when signal impinges upon object with dimensions larger than wavelength of signal)
- Diffraction (Occurs because of an edge or an object, whose size is comparable to the wavelength of the signal)
- Scattering (Occurs when the signal strikes the object with dimensions smaller than the wavelength of the signal)
- Refraction (Bending of the signal due to different refractive indices)
- Attenuation (Amplitude scaling)
- Absorption

The multiple copies at the receiving end may add up destructively or constructively forming an envelope of the signal due to the power level variations. This envelope is characterized by the Rayleigh distribution [12].

## 2.2 PHASE NOISE ANALYSIS FOR OFDM

Every OFDM system is influenced by the difference in the phase as well as frequency of the transmitter and receiver oscillators or in other words, oscillator imperfection [13], hence causing random fluctuations in the phase of transmitted symbol. The carrier recovery at the receiver side plays a vital role in ensuring that the phase of received signal is not altered. If the phase alteration occurs, it violates the orthogonality of subcarriers as well as causes inter-carrier-interference (ICI) [17] in multicarrier systems. This phase alteration is known as phase noise. However, in single-carrier (SC) systems, the phase noise causes signal-to-ratio (SNR) degradation and not inter-symbol-interference (ISI) or ICI. The high sensitivity to the phase noise is a critical drawback observed in OFDM systems, and it arises due to the local oscillators. Due to the presence of phase noise in OFDM, any researcher expects a fall in the performance of the OFDM system as compared to the phase-noise-free-OFDM system [18], [19]. In order to study the effect of phase noise in detail, it is necessary to categorize it initially, because the phase noise influences the OFDM systems in two forms, one which is present within one subcarrier spacing; while, the other one that extends across adjacent subcarrier spacing.

Broadly, the phase noise is known to impact the OFDM system in two forms

1. Common-phase-error (CPE)
2. Inter-carrier-interference (ICI)

CPE causes the phase rotation of the OFDM symbol to be transmitted, and it is common to all subcarriers within a symbol. However, the ICI introduces subcarrier interference due to other subcarriers in that OFDM symbol. It is observed that the ICI component exhibits noise-like behaviour. The CPE is a multiplicative distortion, while ICI is an additive interference.

There are numerous algorithms already proposed to compensate for the phase noise in order to ameliorate the performance of the impaired OFDM system. Before the application of any kind of algorithm, it is important to review the statistics and characterization of the phase noise.

## 2.3 PHASE NOISE MODELLING

Initial step in the analysis of phase-noise-affected OFDM system is to gain prior information about the nature of the phase noise process. This is necessary to implement the algorithms that have been proposed to compensate for the phase noise. Often, two types of models are considered for the phase noise. First, for a phase-locked system, the phase noise is modelled

as zero-mean, stationary random process; and the second, for a frequency-locked system, phase noise is modelled as zero-mean, non-stationary Wiener process. For the purpose of analysis in the prior work and further research, the phase noise is usually modelled as Wiener process [20], [21].

In most of the prior works, the phase noise $\Phi_i$ is modelled as Wiener noise or Brownian motion, and it is represented as

$$\Phi_i = \Phi_{i-1} + u_i, \qquad 0 \le i \le N-1 \tag{2.1}$$

where, $u_i$ denotes the independent and identically distributed (i.i.d.) Gaussian random variable with zero mean and variance $\sigma_u^2$, such that $\Phi_{-1} = 0$ and $\Pr\left(u_i = \pm 1\right) = \frac{1}{2}$.

### 2.3.1 Brownian Motion or Wiener Process

Let us assume that the position of a Brownian particle is computed in one-dimension and the initial position is set to $n = 0$. Therefore, a Brownian stochastic process (standard Wiener process) $\left\{W_n\right\}_{n>0}$ possesses the following characteristics and properties

1. $W_0 = 0$.
2. $W$ has independent and stationary increments/decrements; this denotes time homogeneity as well as spatial homogeneity. Time homogeneity states that the underlying statistics do not vary with time, instead the distribution only depends on the length of the time-interval. Any Brownian motion is characterized by the occurrence of collisions between the particles. If the collision time is small as compared to the time interval between any two collisions, the occurrence is said to be independent.
3. The difference between consecutive random variables $W_n - W_{n-1}$ is Gaussian distributed with zero mean and variance say $\sigma_{ww}^2$. The statement that mean is zero signifies spatial homogeneity i.e., in any collision, it is equally likely that the particle may be jolted to the right or left, hence, rendering the mean of the process to be zero.

2.3.1.1 *Brownian Motion: A Limit of Random Walk*

It is important to discuss this aspect of Brownian motion because of two important reasons. Most of the Brownian stochastic processes exhibit the characteristics of a random walk process for longer durations, with small but recurrent steps. Also, some of the statistics of the random walk may possess limited distributions, which may correspond to Brownian process.

A form of continuous-time stochastic process can be expressed as

$$W_n(t) = \frac{1}{\sqrt{N}} \sum_{i=1}^{nt} u_i \tag{2.2}$$

where, $u_i$ is a sequence of i.i.d. random variables (RVs), which are Gaussian distributed with zero mean and variance 1. Here, $W_n(t)$ is a step function and is random in nature, with a step size of $1/\sqrt{N}$ at times $k/n$; where k is any positive integer. The random variable $u_i$ is such that it may have probability $\Pr(u_i = 1) = \Pr(u_i = -1) = 1/2$. **W** represents the partial sum of these independent and stationary random variable in discrete-time.

It can be summarized that a Brownian motion or in other words, a stochastic process is a scaled form of random-walk process for large occurrences, and it is characterized by the following properties

1. Independence
2. Statistically stationary
3. Gaussian distribution
4. Continuity

## 2.4 PERFORMANCE DEGRADATION OF SYSTEM DUE TO PHASE NOISE

The system performance is usually evaluated in terms of the bit-error-rate (BER), and it has been observed that the presence of phase noise and other frequency errors degrade the BER; and the extent of this degradation has been derived by Pollet *et al.* [22]. The phase noise is modelled as Wiener phase noise. For further simplifications, it is considered to follow a Lorentzian spectrum, and it is equal to $4\pi\beta|t|$; where $\beta$ is the 3-dB line-width of power density of a free-running-oscillator.

The degradation of BER is calculated by comparing the SNR of two scenarios: phase noise present and phase noise absent. The SNR without and with phase noise in the system is given as respectively

$$SNR = \frac{E_s}{N_o} \tag{2.3}$$

$$SNR_{pn} = \frac{E^2}{\frac{N_o}{E_s} + \sigma^2} \tag{2.4}$$

where, $E_s$ is the signal energy, and $N_o$ is the noise power-spectral-density, $E$ represents the power of the useful component, when the system is under the impact of phase noise, $N_o / E_s$ is the variance of thermal noise, and $\sigma^2$ is the variance of all other noise components [22].

Therefore, the BER degradation is given as

$$D_{BER} = -10\log\left(\frac{SNR(with\ phase\ noise)}{SNR(without\ phase\ noise)}\right) \tag{2.5}$$

$$= -10\log\left(\frac{\frac{E^2}{N_o / E_s + \sigma^2}}{E_s / N_o}\right) \tag{2.6}$$

$$D_{BER} = -10\log\left(\frac{E^2}{1 + \sigma^2 \frac{E_s}{N_0}}\right) \tag{2.7}$$

We know that in OFDM, the number of subcarriers is more than 1, say *N;* and consequently, the symbol rate is $R_{OFDM} = N/T$, while in SC systems, it is $R_{SC} = 1/T$. Using the analytics in [22], the degradation in BER can be simplified to

$$D_{BER} = \frac{10}{\ln 10}\frac{11}{60}\left(4\pi N \frac{\beta}{R}\right)\frac{E_s}{N_0} \qquad for\ OFDM \tag{2.8}$$

$$D_{BER} = \frac{10}{\ln 10}\frac{1}{60}\left(4\pi\frac{\beta}{R}\right)\frac{E_s}{N_0} \qquad for\ SC \tag{2.9}$$

## 2.5 PHASE NOISE ESTIMATION AND CORRECTION

OFDM communication systems suffer due to the adverse effects of the phase noise [20]-[23]. Therefore, it is important that the phase noise should be cautiously considered while using OFDM systems in practical applications, like digital-audio-broadcasting (DAB) [7], digital-video-broadcasting (DVB) [8] and high-performance-radio-LAN (HIPERLAN). The phase noise influences the effectiveness of the system in two different ways as discussed in [18] i.e., CPE as well as ICI [24]. In order to improve the degraded system performance, the phase noise needs to be carefully examined for its tolerance limit, so that the design specifications of the OFDM system could be simplified. If the phase noise in the system is assumed to be constant, it can be compensated by the usage of low-complexity correction techniques [22]. Besides, the impact of the phase noise in multi-carrier systems (e.g., in OFDM, which is an MCM using overlapping orthogonal carriers) is observed to be same as in case of the single-carrier systems, when the effects of phase noise are not corrected or suppressed using any compensation technique [23].

In the literature, some of the algorithms or techniques directly evaluate the phase noise and mitigate its effect by compensating for CPE and ICI, while some of the approaches used do so in the time-domain. Therefore, the techniques that may be utilized to mitigate the effect of the phase noise can be classified into two broad classes depending on the operating domain i.e., time-domain approaches and frequency-domain approaches.

- Time-domain Approaches: In these techniques, the common-phase-error component i.e., the multiplicative phase noise is corrected before the DFT-operation by using a single pilot subcarrier from an OFDM symbol, and this is done for every OFDM symbol. This is done to drive a phase-locked-loop (PLL) in the mitigation of the phase noise [25].
- Frequency-domain Approaches: These approaches process the signal to estimate and correct the common phase error and intercarrier interference after the DFT operation.

The frequency-domain approaches are more appropriate practically, as they do not consider the pilot pattern or the characterization of channel environment; whereas the time-domain approaches require a specific pilot pattern, as the pilots are inserted in the middle of the bandwidth, hence making them complex in practice.

Some of the techniques that have been proposed in the literature are discussed below. Practically, out of the total number of subcarriers, some of them are allocated for the pilot data, which can also be used for synchronization. The techniques can also be classified as pilot-based or blind methods (no pilot symbols). As it is clear from the name itself, the pilot based techniques make use of the pilot data symbols to achieve the purpose, while the blind schemes use the previously detected symbols.

### 2.5.1 Pilot-based Techniques

It is well known that the pilot symbols are used to analyse the channel variations, frequency error estimation etc. They have been quite often used in the OFDM symbol block, and therefore the compensation of phase noise in underlying OFDM system is different from the blind methods. Some of these are discussed below.

#### 2.5.1.1 *Phase Noise Suppression Algorithm*

OFDM systems perform poorly when the effects of the phase noise are not eliminated. The Wiener phase noise, whose effect has been elaborated in [22], affects the system in a much more complex way than the frequency offset (another anomaly in OFDM systems), which causes a shift in the radio-frequency (RF) and is also needed to be corrected [26], [27]. The phase noise rotates the constellation (due to CPE) and adds crosstalk between the adjacent subcarriers (ICI), hence making the system practically unacceptable. The phase-noise-suppression (PNS) algorithm [28] has been particularly proposed for IEEE 802.11a standard [15], therefore, the data to be transmitted is constructed in accordance with the standard. This PNS algorithm is evaluated for the Rayleigh fading environment [12]. It utilizes null and pilot symbols. The crux of the algorithm is that it estimates the common phase error component as well as the ICI statistical parameters. These estimates are utilized for the data detection by using minimum-mean-square-error (MMSE) detector. The equalization technique coefficients are in turn calculated using the estimates obtained in the initial step of the algorithm. The estimate of the common phase error is updated after every iteration using the decision feedback. This algorithm is repeated step-by-step for all the OFDM symbols.

This algorithm has been analyzed through MatLab simulation trials, and it is observed that it provides excellent results for the low-complexity computations. The performance has been compared with the phase noise compensation in [24], and it has been observed that the PNS algorithm for IEEE 802.11a standard showcases better performance. And this implies that PNS algorithm is very effective in elimination of the error floor of receiver performance

in OFDM systems caused by the phase noise. It can be inferred from the numerical analysis of the PNS algorithm that its performance is in accordance with the analytical results, and the phase noise is eliminated to a large extent. It outperforms other conventional techniques for various phase noise conditions, and it also demonstrates a behaviour that is very close to the no phase noise in OFDM scenario.

#### 2.5.1.2 *Windowing and Self-ICI Cancellation*

The OFDM systems are prone to frequency errors [14], like carrier frequency offset, phase noise and I/Q imbalance. The common phase error can be easily eliminated (estimated and suppressed), but ICI resulting from frequency error requires complex methods for the same. Many techniques have been proposed to reduce the errors caused by ICI in particular for a Nyquist channel (that satisfies Nyquist criteria), like windowing and self-ICI cancellation techniques. Gudmundson and Anderson have discussed Windowing methods in [29], used in vast applications that can be grouped in two broad categories. One group comprises of applications that are sensitive to the linear distortion and the second comprises of those, which are sensitive to frequency errors. The applications that are sensitive to linear distortion, windowing method shapes the signal, and it is further cyclically extended at the output of DFT operation. However, the original signal remains unaltered. While, for applications affected by frequency errors, windows like Hanning window (which satisfy Nyquist criteria) are helpful in eliminating the ICI from the signal. Nevertheless, Kaiser window has also shown some satisfactory results in reducing the frequency errors.

The self-ICI cancellation techniques use the weighting coefficients in the algorithm to reduce ICI. As discussed by Armstrong in [30], it is beneficial to map the incoming data onto the adjacent subcarriers in pairs and as a result the ICI becomes dependent on the difference between adjacent coefficients rather than a single weighting coefficient. A substantial reduction in ICI is obtained as a result of this difference, although the value is small. The only major drawback is that only half of the values are transmitted, and therefore it is not bandwidth efficient. Nevertheless, they provide some satisfactory results.

2.5.1.3 *Receiver Algorithms Based on Data Detection Techniques*

Certain receiver algorithms have been proposed and discussed by Munier *et al.* in [31] based on the OFDM symbol observations by utilizing the pilot positions. These allow the pilot positions to spread out, and hence the actual information transmitted or in other words, payload increases. Two algorithms are discussed here.

- First algorithm uses minimum-mean-square-error (MMSE) estimation theory to compensate for the phase noise effects considering the statistical properties.
- In second algorithm, the phase noise term is expanded using power series. The coefficients of the expanded power series are estimated using the maximum-likelihood (ML) criterion.

On comparing these two algorithms, we observe that the maximum-likelihood-sequence-detection (MLSD) seems to be complex in terms of implementation. Nevertheless, the performance evaluated in terms of BER illustrates that the power series algorithm outperforms the MMSE-estimation, if the complexity issue is ignored. If the complexity of implementation is of great concern, then MMSE-estimation demonstrates satisfactory behaviour, and significant gain is observed as compared to the conventional phase noise correction techniques.

2.5.1.4 *Reduction of Phase Noise Using Phase-Locked-Loop (PLL)*

A phase-locked-loop (PLL) is used to constantly adjust the phase of the output signal in accordance with the phase of the input signal. When phase-locked loop is applied to the receiver of an OFDM system affected by phase noise, it yields better performance in comparison to a system where the receiver output is dependent on the filter bandwidth and feedback gain etc., as discussed by in a survey paper by Mir and Buttar in [32]. When the phase noise is modelled as the Gaussian random process with zero-mean in PLL receiver, its variance is found to be less than that of the free-running oscillator. A PLL circuit on the receiver side always locks the original phase with the negative feedback of the phase error. Therefore, for the frequency errors resulting from reference carrier at the transmitter side, the receiver PLL circuit helps in limiting the ICI component. This is achieved by shaping the phase noise power spectral density, which is controlled by the cut-off frequency.

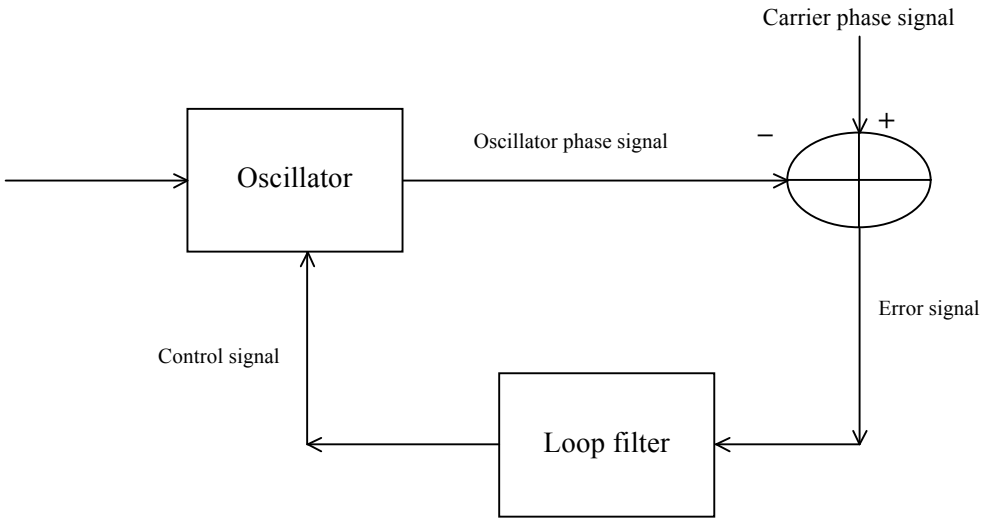


Figure 2.1 A phase-locked loop circuit

2.5.1.5 *Conventional Common-Phase-Error (CPE) Correction (CPEC)*

The common-phase-error comprises of amplitude and a phase. This conventional scheme estimates the phase of CPE rather than the amplitude and phase as in [33]. This is because, when the phase noise is small, the amplitude can be considered to be unity, and hence the significant component is the phase of CPE. This reduces the computational complexity, as only phase has to be calculated from the pilot symbols. The random nature of phase noise also introduces channel estimation errors, and this method of estimation has shown satisfactory performance in reducing these errors as well.

The common-phase-error can be represented as $\alpha e^{j\theta}$, where $\alpha$ represents the amplitude of CPE, while $\theta$ denotes the phase of the same. The CPEC receiver adds pilot tones to the OFDM symbol for the purpose of obtaining rather some optimistic results, if not perfect. The first step at the receiver side is to multiply the received OFDM symbol impaired by phase noise by $e^{-j\theta}$, and consequently, the ICI component is evaluated with this new factor, in which the phase of the CPE is corrected. One point that has to be noted is that the CPEC receiver only performs well when phase noise is slow. In case of fast phase noise, the CPEC receiver is futile.

2.5.1.6 *Pilot-based Channel and Phase Noise Estimation*

This scheme proposed by Zou and Sayed in [34] comprises of two steps or stages, first is the channel estimation (i.e., it has been assumed that channel-state-information (CSI) is not available at the receiver side) and second is the data transmission stage. The pilot-based-OFDM symbol block is transmitted and the receiver makes an estimate of the channel as well as the phase noise simultaneously. This constitutes the first stage of the algorithm. It is noteworthy that the channel coefficient estimation as well as the phase noise error estimation is performed in time-domain rather than frequency-domain. This reduces the computations involved in finding the unknown parameters. This channel estimation is used in the subsequent stage for data detection. In this second stage, the data as well as pilot symbols are transmitted; and at the receiver end, phase noise (CPE and ICI) and data both are estimated. This proposed algorithm may outperform the existing techniques because, unlike other techniques, it evaluates the ICI component instead of just approximating it as an additive-noise term. Another plus point is that it treats the phase noise as unknown parameter instead of making any sort of assumption in its regard. Linear interpolation is used to make estimates of the phase noise making it less prone to errors that may arise due to variations in the phase noise. It is evident from the simulation results provided in [34] that the scheme is quite effective in improving the performance of underlying system. This performance is evaluated in terms of SNR and BER.

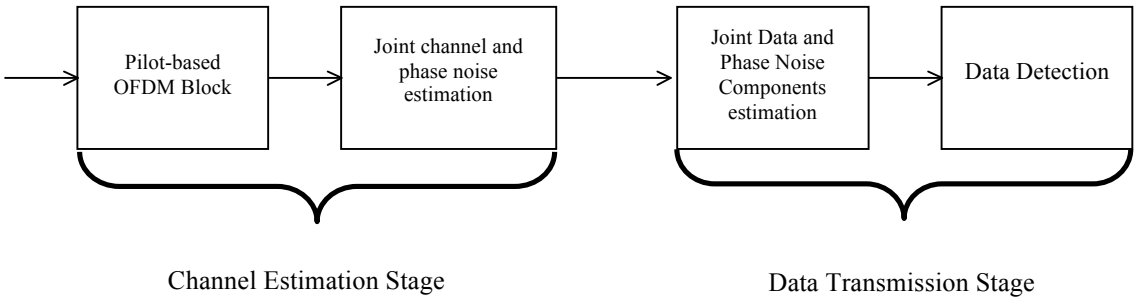


Figure 2.2 Proposed two-stage algorithm for phase noise compensation [34]

2.5.2 Blind Phase Noise Estimation Techniques

We have already discussed the existing research work available in literature in the domain of pilot based phase noise estimation and correction or suppression techniques. The word blind refers to the absence of any pilot symbol or training symbol. Practically, the OFDM symbols are sent by adding pilot symbol, but exceptionally there exists some standards, where the

pilot symbols are not employed. For example, in the very famous WiMAX technology, every third transmitted OFDM symbol is devoid of pilots. As a result, few blind methods have been suggested for the same.

#### 2.5.2.1 *Blind CPE Decision-Directed Algorithm with Decision Uncertainty*

The need for a blind scheme for estimating phase noise, when pilot symbols are absent, led to a proposal of blind decision-directed technique for compensation of phase noise by Sridharan and Lim in [35]. It has been already established that all the symbols are not equally susceptible to errors. Broadly, in this algorithm, the symbols are assumed to be either prone to AWGN or phase noise. Depending upon these two effects, a probability of correct-detection of symbols is derived in [35], hence making it easier to identify the reliable symbols and detecting them using bit-flipping sequential likelihood algorithm. The algorithm first sorts the subcarriers on the basis of their tolerance levels towards phase noise in symbols. The sorting is done in decreasing order. The initial subcarriers are assumed to be correctly detected. As a result, the likelihood function obtained is maximized. This is repeated for all the symbols. This is a decision-directed algorithm, which is vulnerable to decision errors. Irrespective of this, it has shown some acceptable results as presented in [35].

#### 2.5.2.2 *Iterative Receivers Based on Subblock Processing*

Lee and Yang have proposed an iterative algorithm that uses decision feedback to mitigate the effects of ICI in OFDM systems affected by phase noise [36]. This algorithm is based on iterations, and unlike the prior techniques; it does not require any matrix inversion or correlation among DFT coefficients. This reduces the complexity related to implementation. The performance of the algorithm is analysed in terms of signal-to-interference-noise-ratio, whose expressions are also derived in [36] after correcting the phase noise. The first iteration of the algorithm is to estimate the CPE, and perform one-tap equalization as well as decoding. After the first iteration, the OFDM symbol block is subdivided into say, $N_{\mathbf{B}}$ number of subblocks each of size $S = N/N_{\mathbf{B}}$. Then, the estimated time-average of the phase noise in the time-domain at every subblock is used to compensate for the effect of phase noise in each subblock. This algorithm is quite effective in mitigating ICI in comparison to other techniques, and this is illustrated through the simulation results of SINR w.r.t. SNR, as provided in [36].

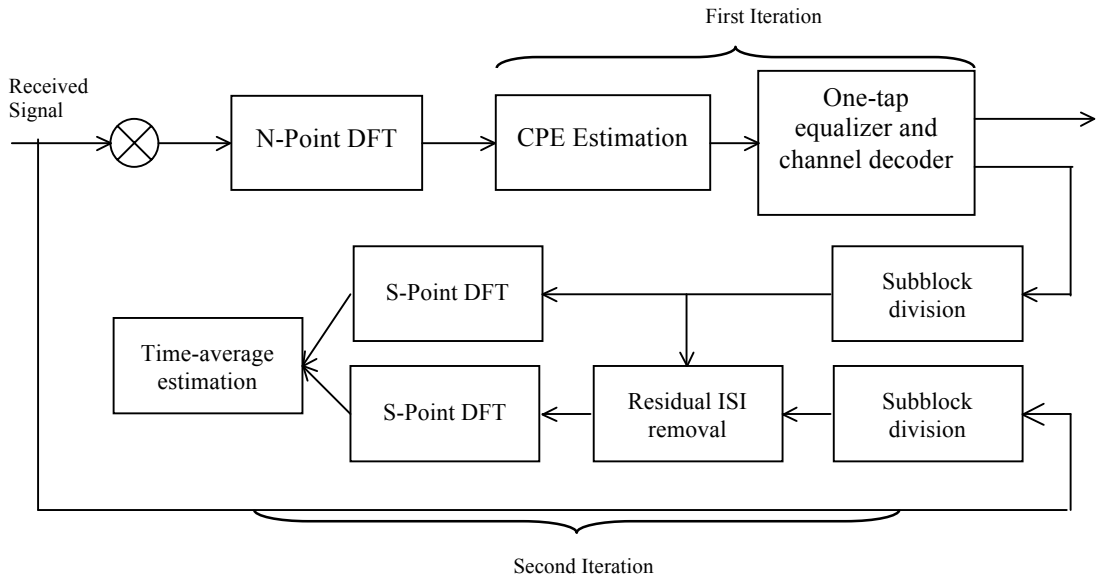


Figure 2.3 Iterative receivers with subblock processing for phase noise compensation

2.5.2.3 *Blind Phase Noise Compensation Technique*

Lee *et al.*, [38] have reported a blind procedure for phase noise compensation, in which single OFDM symbol block is segregated into subblocks, to approximate the time-average of phase noise over every subblock. This time-averaged phase noise and N-point DFT possess an important relation with the OFDM symbol and channel gain [38]. Based on this relation, the estimated phase noise in this single OFDM symbol block duration is used to compensate for the CPE along with ICI mitigation. However under deleterious conditions, the jammer noise may be present to adversely affect the BER performance of the underlying orthogonal frequency division multiplexing system, in combination with additive-white-Gaussian-noise (AWGN).

2.5.2.4 *Low-Complexity Blind Compensation for Phase Noise*

It is a well-established fact for now that the common-phase-noise error rotates the constellation points by a certain angle. If the amount by which the constellation is rotated exceeds a certain threshold value, then the detection of the symbols by compensating the effect of phase noise becomes much more complicated than in usual scenarios. The threshold angles are set according to the constellation of the modulation technique. In [37], as proposed by Hossain *et al.* at a specific constellation point, angles of all the signals are evaluated w.r.t. a reference axis and averaged. The averaged angle is compared to the ideal angle. This process is repeated for all the OFDM signals and averaged. This average value is used to

estimate CPE. It has been assumed in context to the algorithm that the frequency synthesizer is a major source of phase noise. To reduce the complexity, the receiver phase noise is considered for the analysis, and quite satisfactory results have been achieved. The angle of signals at a constellation point can be found by first dividing the constellation on the whole into 4 quadrants, and then the maximum amplitude signal out of the four outputs is detected. Once it is done, the average at every constellation point is calculated. The CPE is obtained by averaging the individual CPE angles at *M*-constellation points, which in turn are a result of comparison of ideal and calculated angle.

# CHAPTER-3

# PHASE NOISE COMPENSATION IN THE PRESENCE OF JAMMER NOISE IN OFDM SYSTEMS

---

*In this chapter, we present the analytical formulation of an OFDM communication link hindered by transmitter and receiver phase noise as well as jammer noise. The prime focus is on compensating the effects of phase noise. The algorithms used for the purpose can be broadly classified into two categories, one based on pilot symbols and the other one blind algorithms. Here, we model the underlying OFDM system for phase noise compensation using the blind algorithm to estimate the effects of phase noise. The efficacy of the algorithm is evaluated in terms of bit error rate. Simulation trials are performed to validate the analytic deductions or interpretations, and the corresponding results are presented in this chapter.*

---

## 3.1 INTRODUCTION

It has been seen in the literature survey that phase noise influences the system in a negative way and degrades the performance of the system. So it becomes necessary to negate its adverse effects. An OFDM system can also be affected by jammer noise from unknown sources. Such a system is not practically acceptable, since the BER performance is very low. In order to make the system acceptable, we tend to reduce the effects of phase noise and the jammer noise. Since jammer noise may be from sources that are unintended, it may be a difficult approach to stabilize the system performance. Another way to achieve this is to compensate the effects of the phase noise. There are certain techniques that have been proposed and used in applications to cancel out the effect of phase noise. Most of the proposed techniques use pilot symbols, but for the phase noise analysis, it is preferred that the pilot symbols are not employed. Such techniques are termed as blind compensation algorithms. One such algorithm, proposed by Lee *et al.* in [38], makes similar assumptions. This algorithm compensates for the effect of phase noise at the subblock level by computing time-average of the phase noise for every subblock. It is a low-complexity technique, but it is applicable to only selective scenarios. Irrespective of the above conditions, this technique shows better performance as compared to other techniques like constrained-minimum-mean-square-prediction-error (C-MMPSE) [41]. In order to use this technique in OFDM systems that are under the impact of the jammer noise, we evaluate its efficacy for various scenarios for a system model, impaired by phase noise as well as jammer noise. This chapter presents

the underlying system model and the results of simulation trials performed to examine the effectiveness of the blind phase noise compensation technique for the underlying system.

## 3.2 OFDM SYSTEM MODEL UNDER THE INFLUENCE OF JAMMER NOISE

The most promising digital modulation in this fast growing communication industry is OFDM [14]. The communication link in this case makes use of OFDM modulation technique. The information in OFDM is encased using cardinal sine functions, and it is achieved using the advance digital signal processing. Here, we provide an overview of the functionality of the OFDM modulation and demodulation. We observe that, the front-end of the communication link, which is analog in nature, is a crucial source of noise because it consists of oscillator device, as well as the channel may contain some intended or unintended sources of jammer noise. A key relationship, that has to be derived, is between the transmitted and the received OFDM symbol block, keeping the effects of the jammer noise and the phase noise in mind. OFDM modulator transmits information in the form of bursts. These bursts are known as OFDM symbols, where each OFDM symbol carries *N* information symbols.

### 3.2.1 Transmitter

The time duration of an OFDM symbol is $T_s$ seconds, and as a result, the system bandwidth can be given as $BW = N / T_s$. The input to *N*-point inverse-discrete-Fourier-transform (IDFT) operation is an OFDM symbol block of size $N \times 1$ represented as $\vec{\mathbf{X}} = \left[X_0, X_1, ..., X_{N-1}\right]^T$, where $\left[.\right]^T$ represents the matrix transpose operation, *N* is number of subcarriers in single OFDM symbol, and $X_k$ denotes the constant modulus modulated data transmitted on the *k*th subcarrier, where $\left|X_k\right|^2 = E_X$ for all *k*. Due to the normalized inverse-DFT operation at transmitter, the time-domain sample vector hence obtained is given as $\vec{\mathbf{x}} = \left[x_0, x_1, ..., x_{N-1}\right]^T$. Using IDFT operation, the symbols are mapped to sinusoidal i.e., sine and cosine signals, which are orthogonal and in window-exponential form.

### 3.2.2 Multipath Channel

The cyclic-prefix (CP) used in OFDM symbol block helps in eliminating the effects of intersymbol interference. This CP-OFDM symbol sample vector is transmitted through the multipath fading channel (that introduces noise (AWGN) and interference in the OFDM symbol) of length *L*. The multipath channel in the underlying OFDM system model follows Rayleigh distribution. It is assumed that the channel state information remains constant during an OFDM symbol block period, and it is perfectly known at the receiver. It is noteworthy that besides AWGN, the transmitted OFDM signal may be affected by the jammer noise from an intended or unintended source.

### 3.2.3 Receiver

It is noteworthy that besides AWGN, the transmitted OFDM signal may be adversely affected by the jammer noise. Hence, the data sample $y_i$ received at any time instant *i*, after propagating through a multipath channel and removal of CP, is written as

$$y_i = \exp\left(j\Phi_i\right)\sum_{l=0}^{L-1} h_l x_{\langle i-l\rangle_N} + \left\{w_i + \eta_i\right\}, \qquad 0 \le i \le N-1 \tag{3.1}$$

where, $\Phi_i$ denotes the phase noise at time instant *i*, $\left\{h_l\right\}_{l=0}^{L-1}$ represent the channel impulse response coefficients of length *L*, and $\left\langle . \right\rangle_N$ indicates the modulo-*N* operation. Here, $w_i$ is the AWGN component, which is independent and identically distributed complex random variable with zero-mean and variance $\sigma_w^2$; and $\eta_i$ denotes the jammer noise at time instant *i*. The nature of jammer noise is assumed to be unknown in the time-domain, implying that it may possess any probability density function, while exhibiting zero-mean and variance $\sigma_\eta^2$.

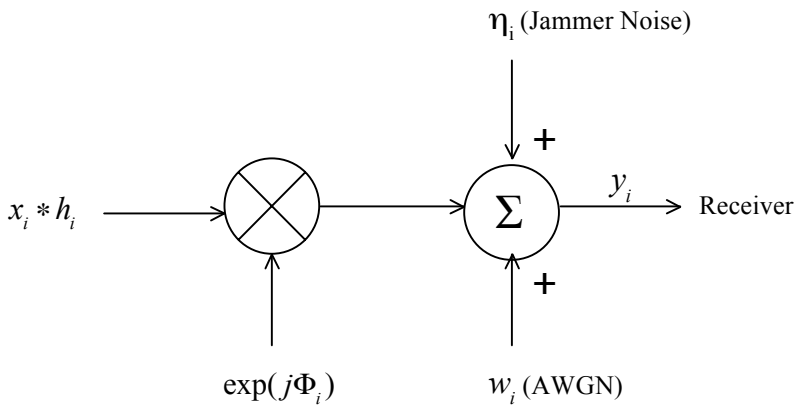


Figure 3.1 Time-domain OFDM signal reception (CP not shown)

The phase noise $\Phi_i$ is modelled as Brownian motion or Wiener process [20],

$$\Phi_i = \Phi_{i-1} + u_i, \qquad 0 \le i \le N-1 \tag{3.2}$$

where, $u_i$ is the Gaussian distributed random variable with zero-mean and $\sigma_u^2$ variance. $\Phi_{-1}$ is assumed to be zero considering perfect synchronization at the starting point of the initial OFDM symbol block. Taking $N$-point DFT of the received signal $y_i$ in Equation (3.1), we obtain

$$Y_k = \left\{H_k X_k J_0\right\} + \left\{\sum_{n=0, n\neq k}^{N-1} H_n X_n J_{k-n}\right\} + \left\{W_k + \Lambda_k\right\}, \qquad 0 \le k \le N-1 \tag{3.3}$$

where, $H_k$ denotes the channel gain at the $k$th subcarrier in frequency-domain, $W_k$ and $\Lambda_k$ are the $k$th normalized $N$-point DFT coefficients of $\left\{\exp\left(jw_i\right)\right\}_{i=0}^{N-1}$ and $\left\{\exp\left(j\eta_i\right)\right\}_{i=0}^{N-1}$ respectively. Here, $\Lambda_k$ is the Gaussian distributed random variable with zero-mean and variance $\sigma_\eta^2$. The Gaussian distribution of $\Lambda_k$ in the frequency-domain is in close agreement with the noise bucket effect [39]. The discrete-time channel gain of length $L$ in frequency-domain can be expressed as

$$H_k = \sum_{l=0}^{L-1} h_l \exp\left(-j\frac{2\pi lk}{N}\right), \qquad 0 \le k \le N-1 \tag{3.4}$$

However, $J_0$ represents the common phase error [28] and $J_k$ is given as [38],

$$J_k = \frac{1}{N}\sum_{i=0}^{N-1} \exp\left(j\Phi_i\right) \exp\left(-j\frac{2\pi ik}{N}\right), \qquad 0 \le k \le N-1 \tag{3.5}$$

Assuming that a received OFDM symbol block is divided into $B$ number of subblocks in the time-domain and $S$ is the number of samples in one subblock. The time-average of phase noise within $p$th subblock is expressed as

$$\bar{\Phi}_p = \frac{1}{S}\sum_{i=pS}^{pS+S-1}\Phi_i, \qquad 0 \le p \le B-1 \tag{3.6}$$

where, $S = N/B$. The phase noise at $p$th subblock is approximated with its time-average $\bar{\Phi}_p$ as

$$\Phi_{pS+s} \cong \bar{\Phi}_p, \qquad 0 \le s \le S-1 \tag{3.7}$$

The received signal at the $k$th subcarrier, which is now in frequency-domain, is compensated for the effect of phase noise. If the phase noise is known at the receiver, the received OFDM symbol block can be perfectly compensated for the adverse effects of phase noise. It follows that

$$\bar{Y}_k = \frac{1}{\sqrt{N}}\sum_{i=0}^{N-1}\exp\left(-j\Phi_i\right)y_i\exp\left(-j\frac{2\pi ik}{N}\right), \qquad 0 \le k \le N-1 \tag{3.8}$$

$$= H_k X_k + \left\{\bar{W}_k + \bar{\Lambda}_k\right\}, \qquad 0 \le k \le N-1 \tag{3.9}$$

However, if the phase noise is not perfectly known and compensated at the receiving end, it is approximated using time-averages at subblock level. This implies that the received OFDM symbol block can be compensated for the effect of phase noise using these calculated time-averages corresponding to each subblock, and hence the frequency-domain received signal can be expressed as

$$\bar{Y}_k \cong \frac{1}{\sqrt{N}}\sum_{p=0}^{B-1}\sum_{s=0}^{S-1}\exp\left(-j\bar{\Phi}_p\right)y_{pS+s}\exp\left(-j\frac{2\pi\left(pS+s\right)k}{N}\right), \tag{3.10}$$

$$= \sum_{p=0}^{B-1}\exp\left(-j\bar{\Phi}_p\right)\exp\left(-j\frac{2\pi pSk}{N}\right)C_{k,p} \tag{3.11}$$

where, $C_{k,p} = \frac{1}{\sqrt{N}}\sum_{s=0}^{S-1}y_{pS+s}\exp\left(-j\frac{2\pi sk}{N}\right)$ values are computed by applying the $N$-point DFT operation on the received samples with zero-padding at $p$th subblock i.e., $\left[y_{pS}, y_{pS+1}, ..., y_{pS+S-1}, 0, 0..., 0\right]^T$. The power of AWGN and jammer noise becomes almost

negligible in the high signal-to-noise-ratio (SNR) regions, and hence it can be neglected, i.e., if $\left\{\bar{W}_k + \bar{\Lambda}_k\right\} \to 0$, then

$$\bar{Y}_k \approx H_k X_k \tag{3.12}$$

Comparing Equation (3.11) and Equation (3.12), we obtain an important relation between the time-average of phase noise and squared magnitude of tapped-delay line channel gain multiplied by the information symbol at *k*th subcarrier, and it can be given as

$$\left|H_k\right|^2 \left|X_k\right|^2 \cong \left|\sum_{p=0}^{B-1} \exp\left(-j\bar{\Phi}_p\right) \exp\left(-j\frac{2\pi pSk}{N}\right) C_{k,p}\right|^2, \tag{3.13}$$

The next step is to mitigate the effect of the ICI and compensate for CPE, as in [38]. Blind-ICI-mitigator (BIM) estimates the difference $d_p = \bar{\Phi}_p - \bar{\Phi}_0$ i.e., $\hat{d}_p$, where $\bar{\Phi}_0$ is the time-average. In order invoke BIM, we utilize this estimated difference to mitigate ICI as

$$z_{pS+s} = \exp\left(-j\hat{d}_p\right) y_{pS+s}, \qquad 0 \le s \le S-1 \tag{3.14}$$

The residual phase noise (represented by superscript R) is required to obtain the estimate of CPE and residual ICI, and is therefore calculated as

$$\Phi^R_{pS+s} = \Phi_{pS+s} - \hat{d}_p, \qquad 0 \le s \le S-1 \text{ and } 0 \le p \le B-1 \tag{3.15}$$

where, $\hat{d}_0 = 0$.

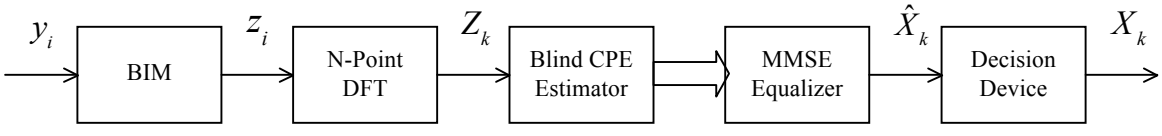


Figure 3.2 Frequency-domain OFDM signal detection using blind CPE estimation

### 3.3 SYMBOL DETECTION IN THE PRESENCE OF JAMMER NOISE

When the deleterious effects of ICI are tried to be eliminated form the received signal sample, a residual phase noise still exists. Therefore, it is necessary to estimate and rectify this residual CPE present in the following

$$Z_k = J_0^R H_k X_k + \bar{D}_k + \overline{W\Lambda_k}, \qquad 0 \le k \le N-1 \tag{3.16}$$

where, $J_0^R = \frac{1}{N}\sum_{i=0}^{N-1} \exp\left(j\Phi_i^R\right) \cong \exp\left(j\bar{\Phi}_0^R\right)$ is the residual CPE, $\bar{D}_k$ is the ICI due to residual phase noise and $\overline{W\Lambda_k}$ are the normalized $N$-point DFT coefficients of $\left\{\exp(j(\Phi_i^R - \Phi_i))(w_i + \eta_i)\right\}_{i=0}^{N-1}$, which are approximated as Gaussian distributed random variables with zero-mean and variance $\sigma_w^2 + \sigma_\eta^2$ (see Appendix A). Based on the observations, the residual CPE $J_0^R$ can be estimated as $\hat{J}_0^R$ by using the phase angle of $Z_k$ w.r.t. $H_k$ (as in [38]) by calculating the phase noise $\hat{\bar{\Phi}}_0^R$. Subsequently, once the residual CPE is estimated, the estimate of the symbol $X_k$ at the $k$th subcarrier can be calculated by using Equation (3.16) as

$$\hat{X}_k = \frac{\left(H_k \hat{J}_0^R\right)^*}{\left|H_k \hat{J}_0^R\right|^2 + \left(\sigma_w^2 + \sigma_\eta^2\right)} Z_k, \qquad 0 \le k \le N-1 \tag{3.17}$$

where, $(.)^*$ represents the complex conjugate operation, and $\hat{J}_0^R = \exp\left(j\hat{\bar{\Phi}}_0^R\right)$ is the estimated residual CPE.

### 3.4 SIMULATION RESULTS

We have already presented an analytic overview of the OFDM system paradigm, impaired by phase noise and under the impact of jammer noise. In order to verify the results obtained through mathematical formulations about the behaviour of the blind algorithm, used to compensate the effect of phase noise in the presence of jammer noise, the simulation trials have been conducted under Rayleigh multipath fading channel conditions. The simulation outcomes provide an insight into the behaviour of the algorithm under adverse conditions and analyze the efficacy of the OFDM system.

The blind algorithm proposed for the phase noise compensation in [38], is validated for its performance using Rayleigh channel conditions and 8-PSK-modulation technique. The number of subcarriers used for the purpose of simulations is 512. It has been proposed in prior research work that the cyclic prefix length should be same or greater than the channel length. So, we chose the CP length of 16, which is used to combat intersymbol interference. The discrete-time multipath frequency-selective channel is modelled as a tapped-delay-line filter with 15-tap coefficients. These channel coefficients are identically and independently Gaussian distributed (i.i.d.) complex random variables; and are assumed to be static during an OFDM symbol period. The frequency-domain Rayleigh fading channel coefficients $H_k$ for $k = 0,\ 1,..., N-1$ are considered to be perfectly known at the receiver. The channel impulse response for each OFDM symbol is randomly generated.

The basic principle of the blind algorithm is to segregate the OFDM block into subblocks in order to analyse the phase noise effects at the subblock level. The number of subblocks is set at $B = 4$ for appropriate compensation of phase noise at the subblock level, which results in suppression of intercarrier interference. For the analysis, the subchannels are mapped using M-ary-PSK-modulation technique. The Monte-Carlo simulation results are obtained by utilizing the ensemble average of 500 trials, while considering different fading channel configurations. It is noteworthy that signal-to-noise-ratio is defined as the ratio of signal power to the AWGN power $\sigma_w^2$.

$$BER_{AVG} = \left. \frac{\sum_{j=1}^{500} BER(j)}{500} \right|_{SNR} \tag{3.18}$$

In order to examine the performance of the underlying system with phase noise and jammer noise, it is assumed for the simulated OFDM systems, that the symbols are perfectly synchronized. The phase noise variations strictly follow the Brownian motion as per a random-walk model. The parameter $\sigma_u$ of the phase noise is varied from 0 to 0.9° at a fixed SNR of +30dB for the different number of subcarriers, and the SNR value is kept +22dB for M-ary PSK digital modulation technique. These results are computed in the presence as well as in the absence of jammer noise in case of phase noise impaired OFDM system. When the jammer noise is assumed to be present, the level of jammer noise power in dB is varied from -35 dB to -10dB. For this case, the parameter $\sigma_u$ of phase noise in Equation (3.2) is fixed at 0.25°.

For the evaluation of performance of the algorithm, we investigate the bit error rate (BER) with respect to the variance of the phase noise (i.e., parameter $\sigma_u$ in Equation (3.2)) and jammer noise power level independently. Broadly, the analysis can be classified into two scenarios, first case being the BER performance with respect to variance of the phase noise and second being the BER performance with respect to the jammer noise level (in dB).

### 3.4.1 Performance Evaluation of Phase Noise Impaired OFDM System Without Jammer Noise

The efficacy of the system for this scenario is evaluated by considering different number of subcarriers and M-ary PSK digital modulation techniques. The blind algorithm used in [38] is evaluated for its performance at $N$ = 512 and 8-PSK modulation. Here, we have considered different number of subcarriers and computed the results for QPSK and 16-PSK as well.

#### 3.4.1.1 *BER vs. Phase Noise Variance (in Degree) for N = 128 and N = 512*

In this case, the phase noise variance is varied by changing the parameter $\sigma_u$ from 0 to 0.9° in Equation (3.2). The performance of blind-phase-noise-compensation (BPNC) technique has been evaluated for $N$ = 128 and $N$ = 512 independently. The digital signal constellation utilized for symbol mapping is 8-PSK at SNR = +30dB. Clearly, it can be observed from Figure 3.3 that the BER performance gets degraded as the variance of the phase noise increases for all values of $N$. We have assumed that the jammer noise is not present in the system. Also, it can be inferred from the Figure 3.3 that the value of BER decreases, as the number of subcarriers increases under similar fading conditions in case of MMSE criterion based data symbol detection. For $\sigma_u = 0.5^\circ$, when number of subcarriers, $N$ changes from 128 to 512, the BER decreases from 0.0233 to 0.0038 (approximate values). Also, at $\sigma_u = 0.75^\circ$, when $N$ = 128, the BER is 0.125; while at $N$ = 512, the BER is 0.01 (approximately). It can be concluded from the observations that as the number of subcarriers increases, the BER improves. For a fixed BER of 0.003, it has been observed that the phase noise parameter $\sigma_u$ is approximately 0° for $N$ = 128 and 0.44° for $N$ = 512.

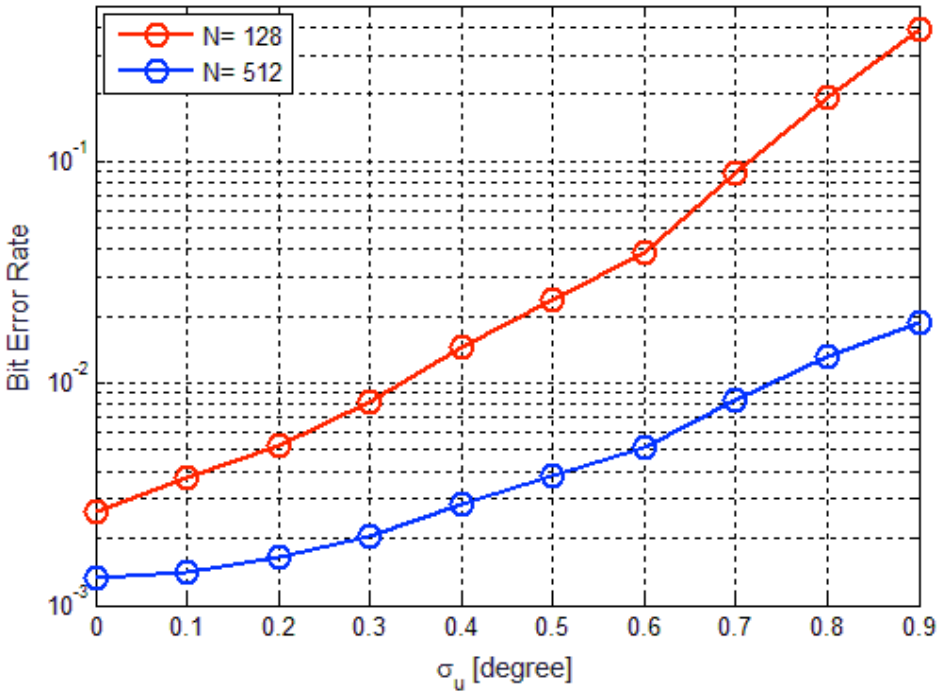


Figure 3.3 BER vs. $\sigma_u$ [degree] at SNR = +30dB for $N$ = 128 and $N$ = 512

| No. of Subcarriers, $N$ | BER at $\sigma_u = 0.5^\circ$ (Approx.) | BER at $\sigma_u = 0.75^\circ$ (Approx.) |
|---|---|---|
| 128 | 0.02333 | 0.125 |
| 512 | 0.003733 | 0.010125 |

Table 3.1 Table Indicating BER at Different Values of Phase Noise Variance for $N$ = 128 and $N$ = 512

3.4.1.2 *BER vs. Phase Noise Variance (in Degree) for N = 256 and N = 2048*

In this case as well, the phase noise variance is varied by changing the parameter $\sigma_u$ from 0 to 0.9° in Equation (3.2). In this case, BER analysis is conducted using $N$ = 256 and $N$ = 2048. The digital signal constellation utilized for symbol mapping is 8-PSK at SNR = +30dB. Clearly, it can be observed from Figure 3.4 that the BER performance gets deteriorated as the variance of the phase noise increases for all values of $N$. We have assumed that the jammer noise is absent in the system. Also, it can be inferred from the Figure 3.4 that the value of BER decreases, as the number of subcarriers increases under similar fading conditions in case of MMSE criterion based data symbol detection. For $\sigma_u = 0.5^\circ$, when number of subcarriers, $N$ changes from 256 to 2048, the BER decreases from 0.0065 to 0.0018 (approximate values).

Also, at $\sigma_u = 0.75^\circ$, when $N$ is changed from 256 to 2048, the BER decreases from 0.0195 to 0.0028 (approximately). It can be concluded from the observation that as the number of subcarriers increases, the BER gets improved. For a fixed BER of 0.003, it is apparent that the phase noise parameter $\sigma_u$ is approximately 0.243° for $N = 256$ and 0.78° for $N = 2048$.

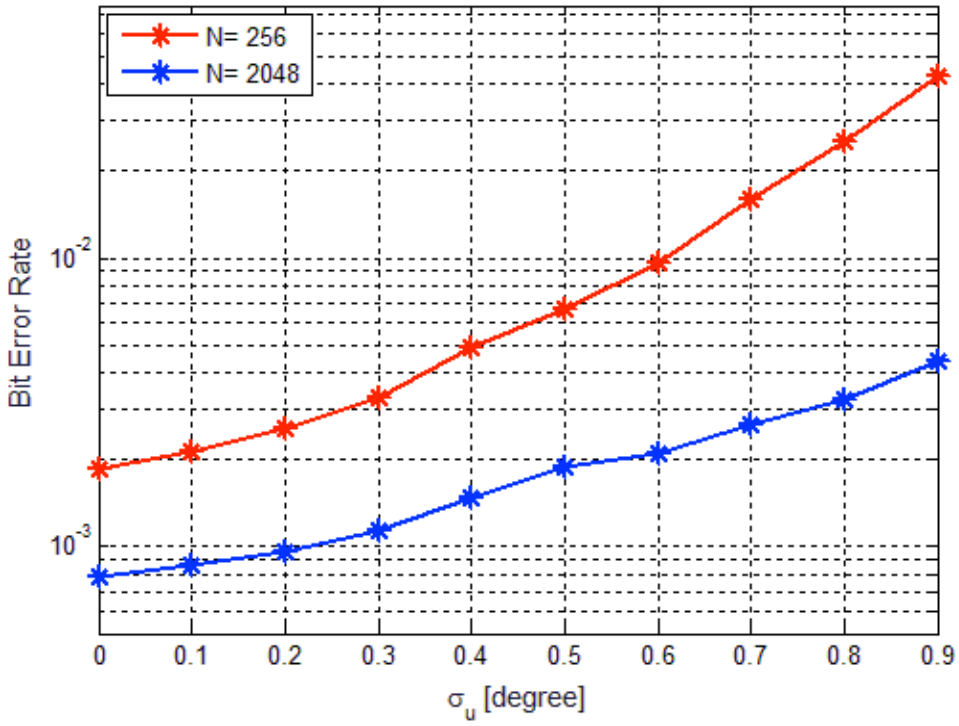


Figure 3.4 BER vs. $\sigma_u$ [degree] at SNR = +30dB for $N = 256$ and $N = 2048$

| No. of Subcarriers, $N$ | BER at $\sigma_u = 0.5^\circ$ (Approx.) | BER at $\sigma_u = 0.75^\circ$ (Approx.) |
|---|---|---|
| 256 | 0.006533 | 0.0195 |
| 2048 | 0.001845 | 0.0028 |

Table 3.2 Table Indicating BER at Different Values of Phase Noise Variance for $N = 256$ and $N = 2048$

Figure 3.5 depicts the overall behaviour of the system for different values of $N$. In this case, the phase noise is varied by changing the parameter $\sigma_u$ from 0 to 0.9°. The number of subcarriers is considered to be $N \rightarrow \{128, 256, 512, 1024, 2048\}$. The digital signal constellation used for symbol mapping is 8-PSK at +30dB SNR. It may be inferred from Figure 3.5 that the BER increases with the increasing value of $\sigma_u$ for all the values of $N$. But

the value of BER decreases, as the number of subcarriers increases under similar fading conditions in case of MMSE criterion based data symbol detection. For $\sigma_u = 0.75^\circ$, when $N$ changes from 1024 to 2048, the BER gets reduced from 0.0056 to 0.0028 (approximate values). It is due to the alleviation of AWGN power per subcarrier at the receiving end.

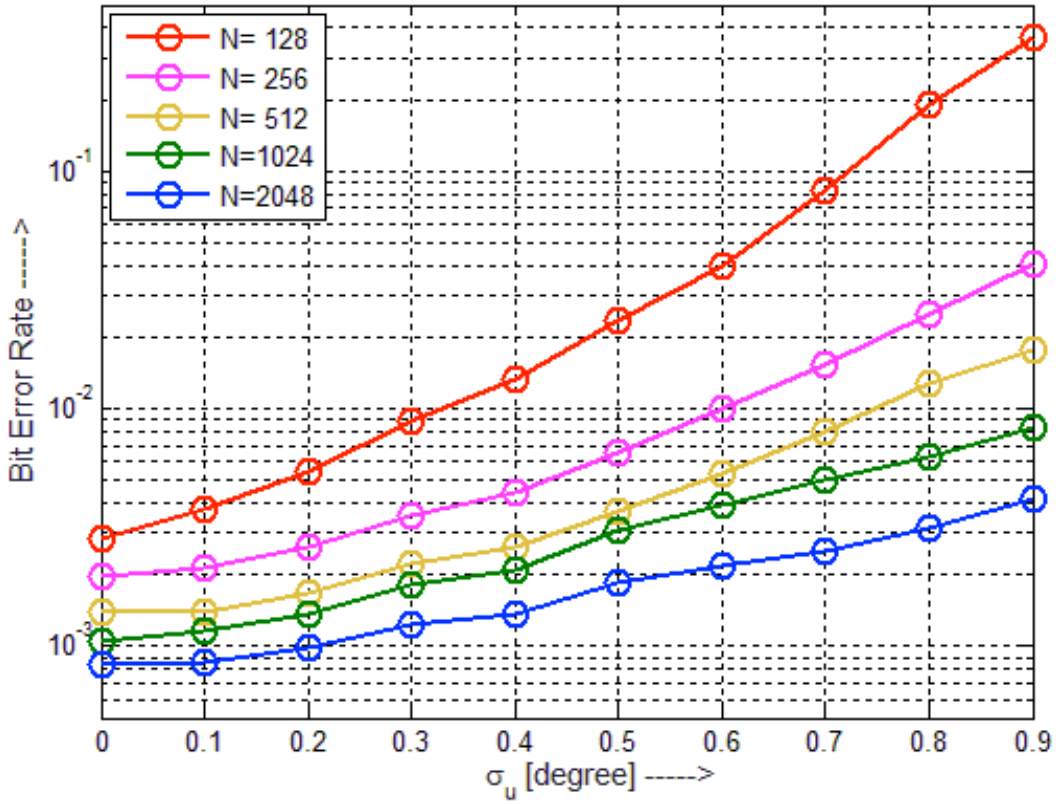


Figure 3.5 BER vs. $\sigma_u$ [degree] at SNR = +30dB for different number of subcarriers

| No. of Subcarriers, $N$ | $\sigma_u$ [degree] (Approx.) |
|---|---|
| 128 | 0 |
| 256 | 0.243 |
| 512 | 0.439 |
| 1024 | 0.494 |
| 2048 | 0.78 |

Table 3.3 Table Indicating $\sigma_u$ w.r.t. $N$ for an OFDM System at BER = 0.003

| No. of Subcarriers, $N$ | BER at $\sigma_u = 0.5^\circ$ (Approx.) | BER at $\sigma_u = 0.75^\circ$ (Approx.) |
|---|---|---|
| 128 | 0.02333 | 0.125 |
| 256 | 0.006533 | 0.0195 |
| 512 | 0.003733 | 0.010125 |
| 1024 | 0.003075 | 0.0056 |
| 2048 | 0.001845 | 0.0028 |

Table 3.4 Table Indicating BER at $\sigma_u = 0.5^\circ$ and $0.75^\circ$ for Different Number of Subcarriers

3.4.1.3 *BER vs. Phase Noise Variance (in Degree) for QPSK and 8-PSK with ZF and MMSE Detectors*

Figure 3.6 presents the simulation results for M-ary PSK digital modulation technique with $M$ = 4 and $M$ = 8. Evidently, it can be seen that as the variance of the phase noise gets elevated, the bit error rate performance degrades for both the modulation schemes. The phase noise parameter $\sigma_u$ in Equation (3.2) is varied from 0 to 0.9°. We have assumed that the SNR is fixed at +22dB and the jammer noise is not present in the system. The number of subcarriers is set at $N$ = 512. We analyze the impact of different constant modulation techniques while comparing the performance of ZF and MMSE detectors. We can observe from the Figure 3.6 that at phase noise parameter $\sigma_u = 0.5^\circ$, the BER decreases from 0.0112 to 0.0026 (approximate values) when the $M$ is changed from 8 to 4 for ZF detector. While, the BER decreases from 0.0098 for 8-PSK to 0.0023 for QPSK (approximate values) when MMSE detector is used. At $\sigma_u = 0.75^\circ$, the BER gets reduced from 0.05 at $M$ = 8 to 0.0058 at $M$ = 4 (approximate values) for ZF detector, and from 0.04 at $M$ = 8 to 0.0046 at $M$ = 4 (approximate values) for MMSE detector. It can also be inferred from the outcomes that MMSE detector performs marginally better than ZF detector.

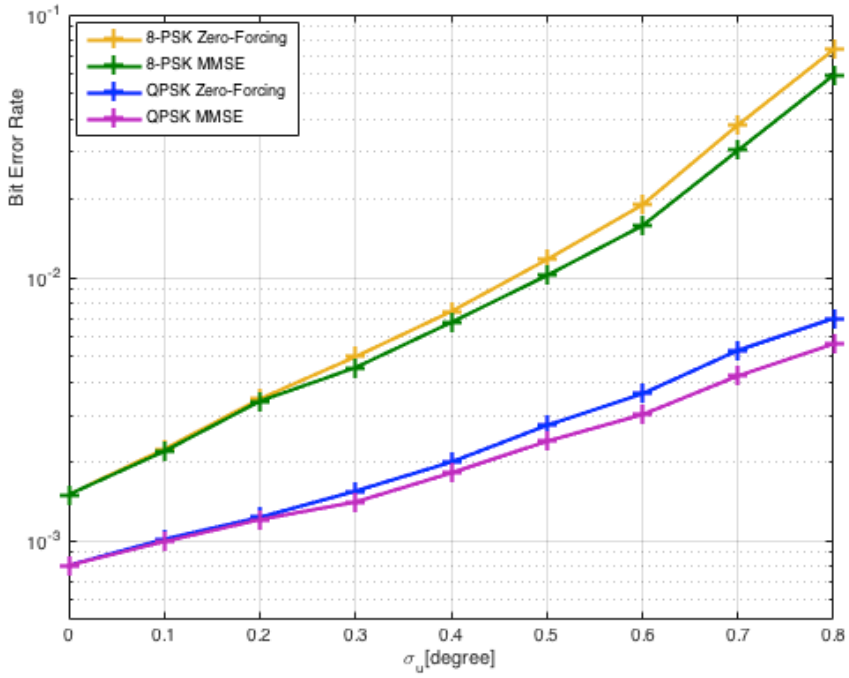


Figure 3.6 BER vs. $\sigma_u$ [degree] at SNR = +22dB for 8-PSK and QPSK (ZF and MMSE detectors)

| Modulation Technique | Type of Detector | BER at $\sigma_u = 0.5^\circ$ (Approx.) | BER at $\sigma_u = 0.75^\circ$ (Approx.) |
|---|---|---|---|
| 8-PSK | ZF | 0.01122 | 0.05 |
| | MMSE | 0.009757 | 0.04 |
| QPSK | ZF | 0.002629 | 0.00575 |
| | MMSE | 0.002286 | 0.004625 |

Table 3.5 Table Indicating BER for 8-PSK and QPSK Digital Modulation Techniques for $N$ = 512 at $\sigma_u = 0.5^\circ$ and $0.75^\circ$

### 3.4.1.4 *BER vs. Phase Noise Variance (in Degree) for QPSK and 16-PSK with ZF and MMSE Detectors*

Figure 3.7 presents the simulation results for M-ary PSK digital modulation technique with $M$ = 4 and $M$ = 16. Evidently, it can be seen that as the variance of the phase noise increases, the bit error rate performance deteriorates for both the modulation schemes. The phase noise parameter is varied from 0 to 0.9° in Equation (3.2). We have assumed that the SNR is fixed at +22dB and the jammer noise is not present in the system. The number of subcarriers is set at $N$ = 512. We analyze the impact of different constant modulation techniques while comparing the performance of ZF and MMSE detectors. We can observe from the Figure 3.7

that at phase noise parameter $\sigma_u = 0.5^\circ$, the BER gets reduced from 0.062 to 0.0026 (approximate values) when the *M* is changed from 16 to 4 for ZF detector. While, the BER decreases from 0.054 for 16-PSK to 0.0023 for QPSK (approximate values) when MMSE detector is utilized. At $\sigma_u = 0.75^\circ$, the BER gets alleviated from 0.24 at *M* = 16 to 0.0058 at *M* = 4 for ZF detector and gets decreased from 0.205 at *M* = 16 to 0.0046 at *M* = 4 (approximate values) for MMSE detector. It can also be inferred from the outcomes that MMSE detector performs marginally better than ZF detector.

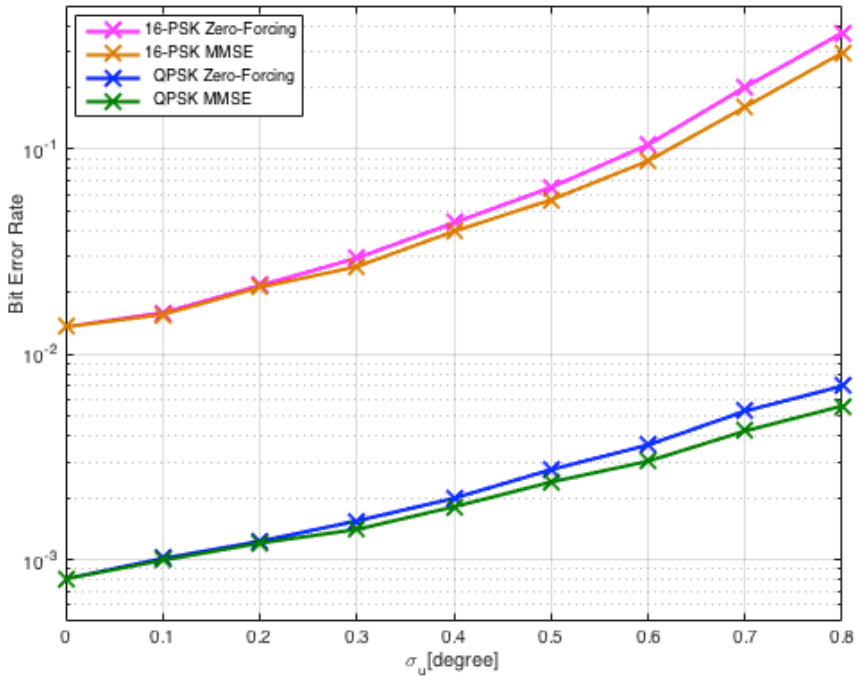


Figure 3.7 BER vs. $\sigma_u$ [degree] for SNR = +22dB for 16-PSK and QPSK (ZF and MMSE detectors)

| Modulation Technique | Type of Detector | BER at $\sigma_u = 0.5^\circ$ (Approx.) | BER at $\sigma_u = 0.75^\circ$ (Approx.) |
|---|---|---|---|
| 16-PSK | ZF | 0.06234 | 0.2575 |
| | MMSE | 0.05421 | 0.205 |
| QPSK | ZF | 0.002629 | 0.00575 |
| | MMSE | 0.002286 | 0.004625 |

Table 3.6 Table Indicating BER for 16-PSK and QPSK Digital Modulation Techniques for *N* = 512 at $\sigma_u = 0.5^\circ$ and $0.75^\circ$

In this case, we kept the SNR +22dB at $N = 512$ for analyzing the impact of different constant modulus modulation techniques, while comparing the performance of ZF and MMSE detectors. For $\sigma_u = 0.75^{\circ}$ and 8-PSK constellation, the BER is observed to be approximately 0.04 in case of MMSE detector and 0.05 in case of ZF detector. As $M$ increases in M-ary PSK from 4 to 16, the Euclidean distance between adjacent constellation points decreases, which leads to elevation in BER value i.e., success rate deteriorates (as shown in Figure 3.8).

Therefore, it may be observed from the results presented in Figure 3.8 that the BER performance of underlying OFDM system gets degraded with the increasing value of $M$ for the fixed value of transmitter power and AWGN power. Moreover, the MMSE detector performs marginally better than ZF detector under similar scenarios.

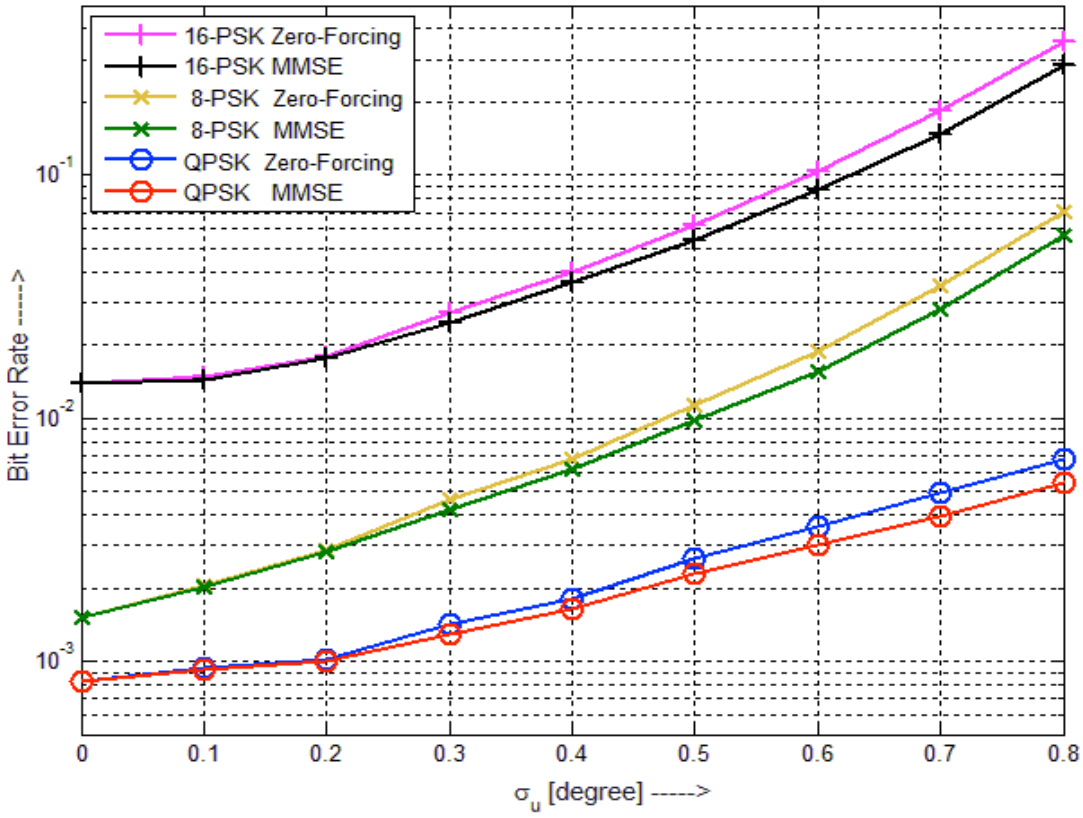


Figure 3.8 BER vs. $\sigma_u$ [degree] at SNR = +22dB for M-ary PSK digital modulation technique

| Modulation Technique | Type of Detector | BER at $\sigma_u = 0.5^\circ$ (Approx.) | BER at $\sigma_u = 0.75^\circ$ (Approx.) |
|---|---|---|---|
| 16-PSK | ZF | 0.06234 | 0.2575 |
| | MMSE | 0.05421 | 0.205 |
| 8-PSK | ZF | 0.01122 | 0.05 |
| | MMSE | 0.009757 | 0.04 |
| QPSK | ZF | 0.002629 | 0.00575 |
| | MMSE | 0.002286 | 0.004625 |

Table 3.7 Table Indicating BER for 16-PSK, 8-PSK and QPSK Digital Modulation Techniques for *N* = 512 at $\sigma_u = 0.5^\circ$ and $0.75^\circ$

### 3.4.2 Performance Evaluation of Phase Noise Impaired OFDM System With Jammer Noise

The jammer noise may originate from any intended or unintended source. The probability distribution function of the jammer noise in time-domain is irrespective because in frequency-domain as a result of DFT operation, the jammer noise power spreads out over all the *N* subcarriers. The behaviour of blind algorithm for this case is also evaluated by considering different number of subcarriers and M-ary PSK digital modulation techniques. The presence of jammer noise increases the BER of the OFDM system, and hence deteriorating the system performance.

#### 3.4.2.1 *BER vs. Jammer Noise Level (in dB) for N = 128 and N = 512*

Figure 3.9 demonstrates the simulation results when jammer noise is present, and for analysing the performance, the number of subcarriers is changed from 128 to 512. We consider the presence of jammer noise with zero-mean and variance $10\log_{10}\sigma_\eta^2$ dB in the time-domain. Undoubtedly, it can be observed that as the variance of the phase noise increases, the bit error rate performance degrades. The phase noise parameter $\sigma_u$ in Equation (3.2) is fixed at a value 0.25°. We incorporate 8-PSK digital modulation technique, while employing MMSE criterion based detector. The SNR is set at +30dB. We vary the power level of jammer noise from -35dB to -15dB and observe the nature of the BER. We can observe from the Figure 3.9, when the jammer noise variance is -30dB; the BER gets alleviated from 0.022 to 0.0065 (approximate values) when the number of subcarriers is

increased from 128 to 512. However, the BER is found to be approximately 0.403 for $N$ = 128 and 0.063 for $N$ = 512, in case the jammer noise variance is -15dB. Therefore, the BER performance deteriorates with the increasing value of jammer noise variance and with the decreasing number of subcarriers for the constant transmitted and total noise (AWGN plus jammer noise) power.

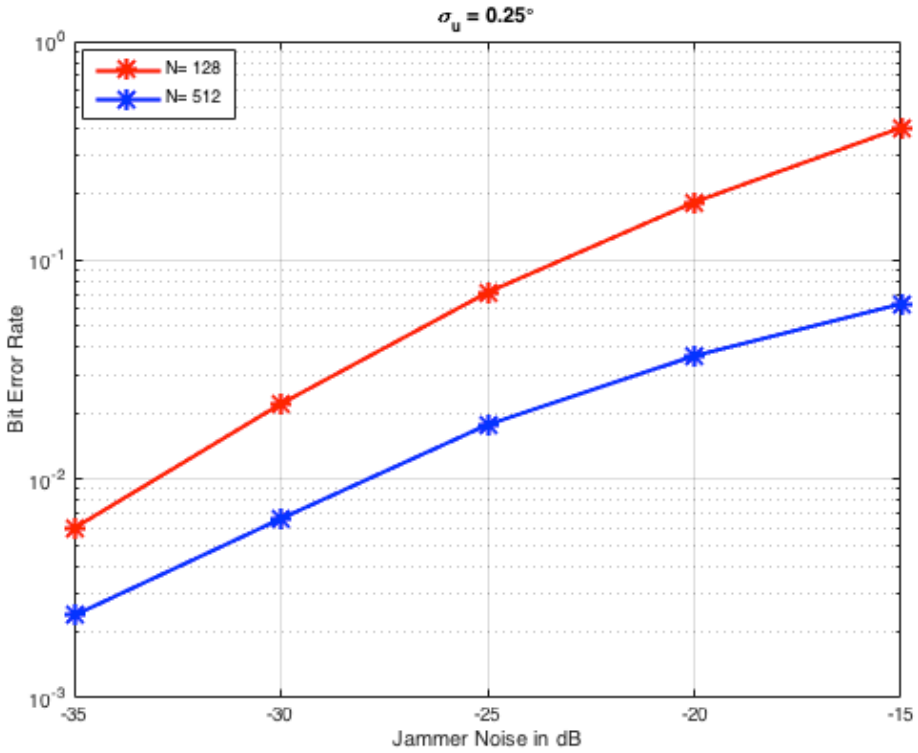


Figure 3.9 BER vs. jammer noise variance (in dB) at SNR = +30dB for $N$ = 128 and $N$ = 512

| No. of Subcarriers, $N$ | BER at Jammer Noise = -30dB (Approx.) | BER at Jammer Noise = -15dB (Approx.) |
|---|---|---|
| 128 | 0.02207 | 0.403 |
| 512 | 0.006592 | 0.06305 |

Table 3.8 Table Indicating BER at Different Levels of Jammer Noise Variance for $N$ = 128 and $N$ = 512 at $\sigma_u = 0.25^{\circ}$

3.4.2.2 *BER vs. Jammer Noise Level (in dB) for N = 256 and N = 2048*

The simulation outcomes, when jammer noise is present, are depicted in Figure 3.10. For analysing the performance, the number of subcarriers is changed from 256 to 2048. We consider the presence of jammer noise with zero-mean and variance $10\log_{10}\sigma_\eta^2$ dB in the

time-domain. Undoubtedly, it can be observed that as the variance of the phase noise elevates, the bit error rate performance gets deteriorated. The phase noise variance parameter $\sigma_u$ is fixed at a value 0.25°. We use 8-PSK digital modulation scheme, while employing MMSE criterion based detector. The SNR is set at +30dB. We vary the power level of jammer noise from -35dB to -15dB and observe the nature of the BER. We can infer from the Figure 3.10 that at jammer noise variance is -30dB, the BER gets reduced from 0.01 to 0.00335 (approximate values) when the number of subcarriers is increased from 256 to 2048. However, the BER is found to be approximately 0.1075 for $N = 256$ and 0.027 for $N = 2048$, in case the jammer noise variance is -15dB. Therefore, the BER performance deteriorates with the increasing value of jammer noise variance and with the decreasing number of subcarriers for the constant transmitted and total noise (AWGN plus jammer noise) power.

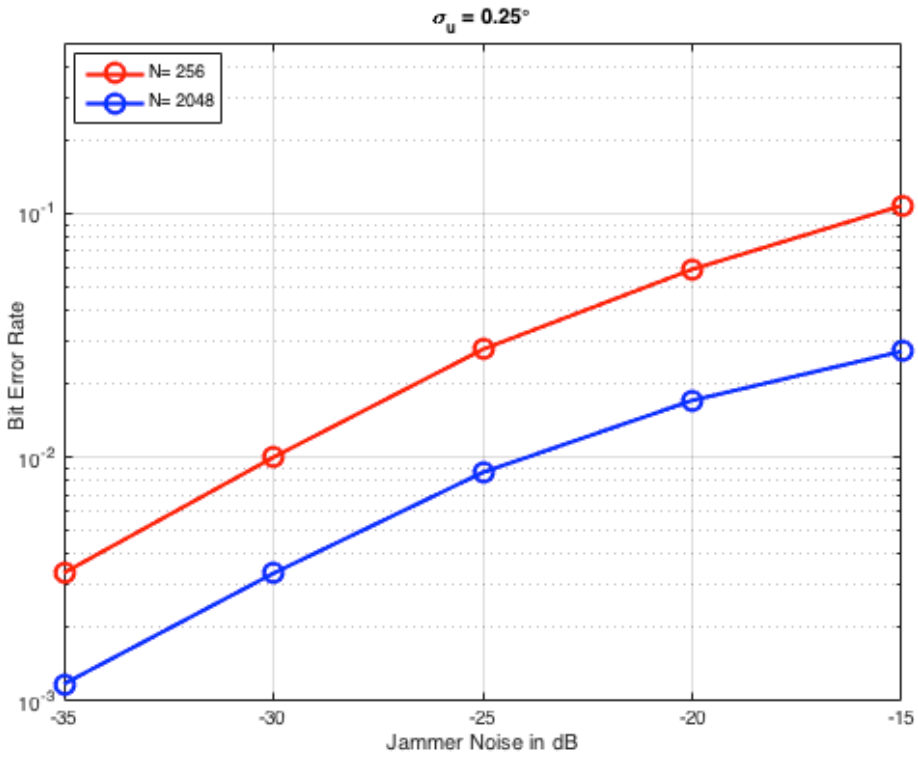


Figure 3.10 BER vs. jammer noise variance (in dB) at SNR = +30dB for $N = 256$ and $N = 2048$

| No. of Subcarriers, $N$ | BER at Jammer Noise = -30dB (Approx.) | BER at Jammer Noise = -15dB (Approx.) |
|---|---|---|
| 256 | 0.01001 | 0.1075 |
| 2048 | 0.003346 | 0.02717 |

Table 3.9 Table Indicating BER at Different Levels of Jammer Noise Variance for $N$ = 256 and $N$ = 2048 at $\sigma_u = 0.25^{\circ}$

In this case, we consider the presence of jammer noise with zero-mean and variance $10\log_{10}\sigma_\eta^2$ dB in the time-domain. The value of parameter $\sigma_u$ is set at 0.25° for the generation of phase noise. We incorporate 8-PSK digital modulation technique, while employing MMSE criterion based detector. The number of subcarriers is considered to be $N \rightarrow \{128, 256, 512, 1024, 2048\}$. The SNR is fixed at +30dB. In the presence of jammer noise with variance -30dB, the BER value is observed to be approximately 0.01 for $N$ = 256 and 0.0066 for $N$ = 512 (as shown in Figure 3.11). However, the BER is found to be approximately 0.051 for $N$ = 1024 and 0.0272 for $N$ = 2048, in case the jammer noise variance is -15dB. Moreover, the BER performance deteriorates with the increasing value of jammer noise variance and with the decreasing number of subcarriers for the constant value of transmitted power and total noise (jammer noise plus AWGN) power. Although, the jammer noise may possess any probability distribution function in the time-domain, yet the DFT operation at the receiver causes the jammer noise power to spread over all the subcarriers leading to the Gaussian distribution in the frequency-domain. This exclusive feature helps BPNC technique based OFDM system to combat jammer noise, while communicating over the multipath fading channels.

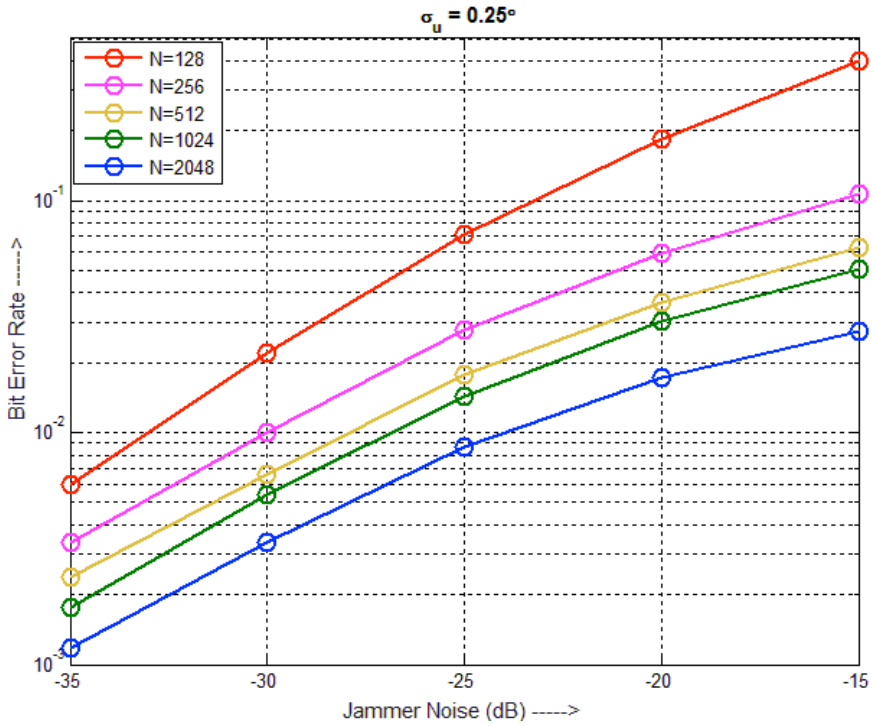


| No. of Subcarriers, *N* | BER at Jammer Noise = -30dB (Approx.) | BER at Jammer Noise = -15dB (Approx.) |
|---|---|---|
| 128 | 0.02207 | 0.403 |
| 256 | 0.01001 | 0.1075 |
| 512 | 0.006592 | 0.06305 |
| 1024 | 0.005426 | 0.05094 |
| 2048 | 0.003346 | 0.02717 |

Table 3.10 Table Indicating BER at Different Levels of Jammer Noise Variance for Different Number of Subcarriers at $\sigma_u = 0.25^\circ$

| No. of Subcarriers, *N* | Jammer Noise (dB) (Approx.) |
|---|---|
| 128 | -33 |
| 256 | -30 |
| 512 | -27.89 |
| 1024 | -26.9 |
| 2048 | -24 |

Table 3.11 Table Indicating Jammer Noise Power Level for Different Number of Subcarriers at BER = 0.01 and $\sigma_u = 0.25^\circ$

3.4.2.3 *BER vs. Jammer Noise Level (in dB) for QPSK and 8-PSK with ZF and MMSE Detectors*

Figure 3.12 presents the simulation outcomes for M-ary PSK digital modulation techniques with $M = 4$ and $M = 8$, assuming that the jammer noise is present. The phase noise parameter $\sigma_u$ is 0.25° in Equation (3.2). We have assumed that the SNR is fixed at +22dB. The number of subcarriers, $N$ is set at 512. It can be inferred from Figure 3.12 that when the jammer noise level is -30dB, the BER while using ZF detector gets reduced from 0.0087 to 0.0039 (approximate values) when the $M$ is changed from 8 to 4. However, when MMSE criterion based detector is used, the BER at the same jammer noise power levels gets alleviated from 0.0085 to 0.00386 (approximate values) when $M$ changes from 8 to 4. Also, from another set of observations given in Table 3.15, we can infer that at BER = 0.02, the jammer noise level is -26.435dB (for ZF detector) and -26.35dB (for MMSE detector) when we incorporate 8-PSK modulation technique; while it is approximately -20.7dB (for ZF detector) and -20.1155 (for MMSE detector) when we incorporate QPSK modulation technique. It is apparent from the simulation results presented in Figure 3.12 that the BER performance of BPNC technique based OFDM system gets degraded with the increasing value of $M$ from 4 to 8, but the MMSE detector performs marginally better than ZF detector in the presence of jammer noise.

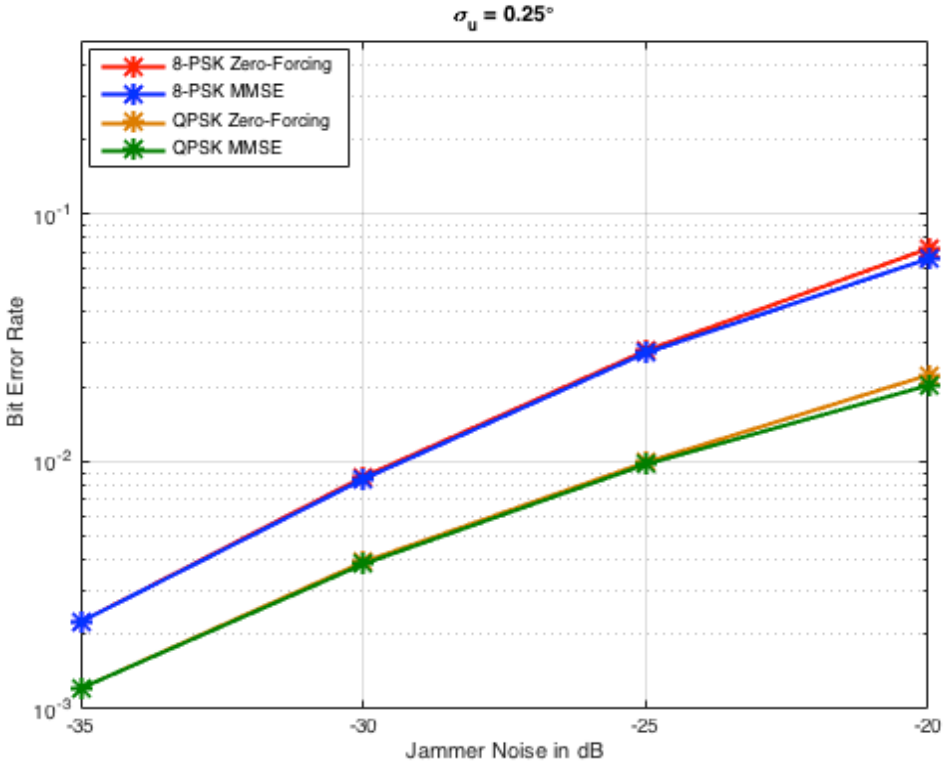


Figure 3.12 BER vs. jammer noise variance (in dB) at SNR = +22dB for 8-PSK and QPSK (ZF and MMSE detectors)

| Modulation Technique | Type of Detector | Bit Error Rate (Approx.) |
|---|---|---|
| 8-PSK | ZF | 0.008679 |
| | MMSE | 0.008508 |
| QPSK | ZF | 0.003937 |
| | MMSE | 0.00386 |

Table 3.12 Table Indicating BER for 8-PSK and QPSK Digital Modulation Techniques when Jammer Noise Variance Level is -30dB ($N$ = 512 and $\sigma_u = 0.25^\circ$)

3.4.2.4 *BER vs. Jammer Noise Level (in dB) for QPSK and 16-PSK with ZF and MMSE Detectors*

Figure 3.13 showcases the simulation results for M-ary PSK digital modulation techniques with $M$ = 4 and $M$ = 16, assuming that the jammer noise is present. The phase noise parameter $\sigma_u$ is 0.25° in Equation (3.2). We have assumed that the SNR is fixed at +22dB. The number of subcarriers, $N$ is set at 512. It can be inferred from Figure 3.13 that when the jammer noise level is -30dB, the BER while using ZF detector gets reduced from 0.062 to 0.0039 (approximate values) when the $M$ is changed from 16 to 4. When MMSE criterion based detector is utilized, the BER at the same jammer noise power levels gets alleviated from 0.061 to 0.00386 (approximate values) when $M$ changes from 16 to 4. Also, from another set of observations given in Table 3.15, it is apparent that at BER = 0.02, the jammer noise variance level is -35dB (for both ZF and MMSE detector) when we incorporate 16-PSK modulation technique; while it is approximately -20.7dB (for ZF detector) and -20.1155 (for MMSE detector) when we incorporate QPSK modulation technique. It is clear from the simulation results presented in Figure 3.13 that the BER performance of BPNC technique based OFDM system gets degraded with the increasing value of $M$ from 4 to 16, but the MMSE detector performs marginally better than ZF detector in the presence of jammer noise.

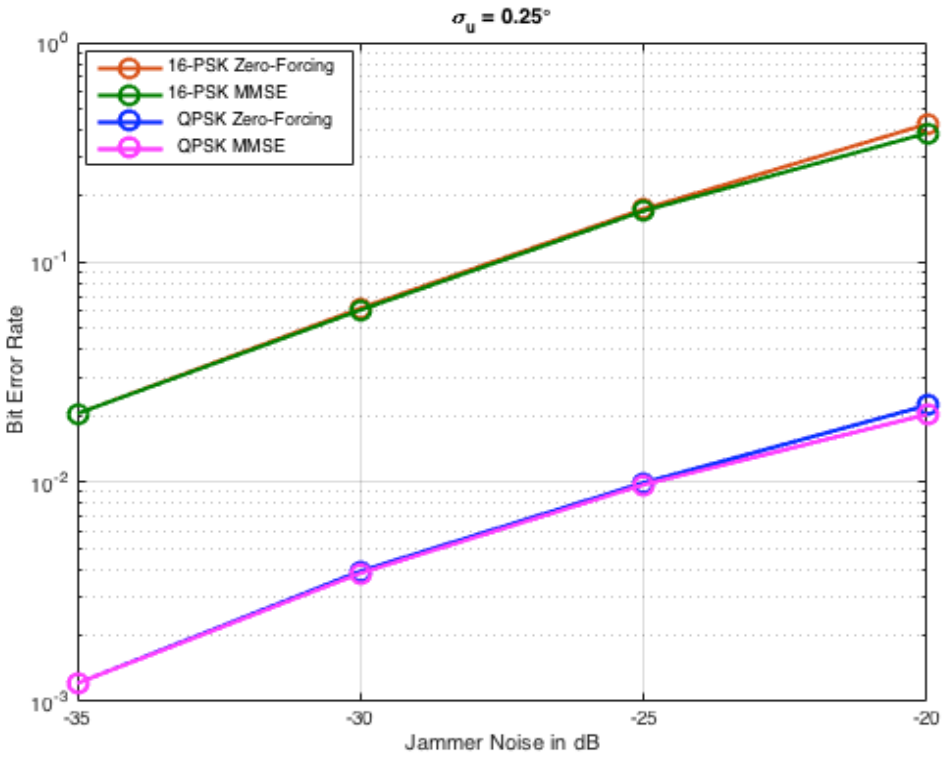


Figure 3.13 BER vs. jammer noise variance (in dB) at SNR = +22dB for 16-PSK and QPSK (ZF and MMSE detectors)

| Modulation Technique | Type of Detector | Bit Error Rate (Approx.) |
|---|---|---|
| 16-PSK | ZF | 0.06199 |
| | MMSE | 0.06077 |
| QPSK | ZF | 0.003937 |
| | MMSE | 0.00386 |

Table 3.13 Table Indicating BER for 16-PSK and QPSK Digital Modulation Techniques when Jammer Noise Variance Level is -30dB ($N$ = 512 and $\sigma_u = 0.25^\circ$)

In this case, we consider the presence of jammer noise with zero-mean and variance $10\log_{10}\sigma_\eta^2$ dB in the time-domain. The value of parameter $\sigma_u$ is set at 0.25° in Equation (3.2) for the generation of phase noise. We incorporate 8-PSK digital modulation technique, while employing ZF as well as MMSE criterion based detector.

Further, the SNR value is set to +22dB for the different types of M-ary PSK digital modulation techniques, at $N = 512$ and $\sigma_u = 0.25^\circ$. It is apparent from the simulation results presented in Figure 3.14 that the BER performance of BPNC technique based OFDM system gets degraded with the increasing value of $M$ from 4 to 16, but the MMSE detector performs marginally better than ZF detector in the presence of jammer noise.

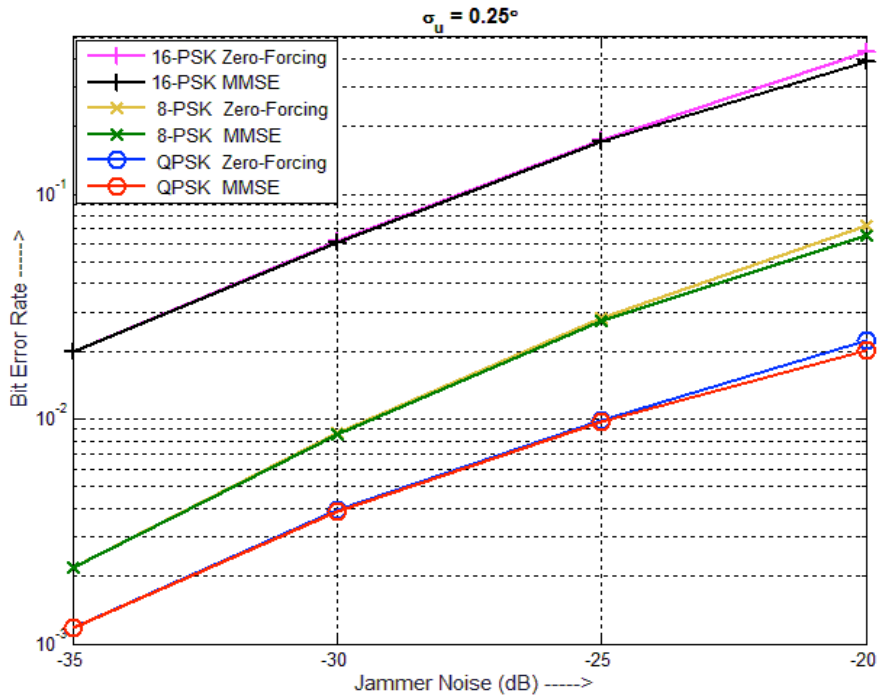


Figure 3.14 BER vs. jammer noise variance (in dB) at SNR = +22dB for M-ary PSK digital modulation technique

| Modulation Technique | Type of Detector | Bit Error Rate (Approx.) |
|---|---|---|
| 16-PSK | ZF | 0.06199 |
| | MMSE | 0.06077 |
| 8-PSK | ZF | 0.008679 |
| | MMSE | 0.008508 |
| QPSK | ZF | 0.003937 |
| | MMSE | 0.00386 |

Table 3.14 Table Indicating BER for M-ary PSK Digital Modulation Techniques when Jammer Noise Variance Level is -30dB ($N = 512$ and $\sigma_u = 0.25^\circ$)

| Modulation Technique | Type of Detector | Jammer Noise (dB) (Approx.) |
|---|---|---|
| 16-PSK | ZF | -35 |
| | MMSE | -35 |
| 8-PSK | ZF | -26.435 |
| | MMSE | -26.35 |
| QPSK | ZF | -20.7 |
| | MMSE | -20.1155 |

Table 3.15 Table Indicating Jammer Noise Variance Level for M-ary PSK Digital Modulation Techniques at BER = 0.02 ($N$ = 512 and $\sigma_u = 0.25^{\circ}$)

Although, the jammer noise may possess any probability distribution function in the time-domain, yet the DFT operation at the receiver causes the jammer noise power to spread over all the subcarriers leading to the Gaussian distribution in the frequency-domain. This exclusive feature helps BPNC technique based OFDM system to combat jammer noise, while communicating over the multipath fading channels.

# CHAPTER-4

# CONCLUDING REMARKS AND FUTURE WORK

The phase noise affects bit error rate performance of OFDM systems in two different ways i.e., due to the common phase error and the intercarrier interference. Several techniques have been proposed in the past in order to nullify the effects of phase noise. The presented research work in this dissertation emphasizes on one such technique i.e., the blind-phase-noise-compensation (BPNC). The bit error rate performance of the blind phase noise compensation method based OFDM system is investigated further for the different number of subcarriers or length of OFDM symbol block, for the different M-ary PSK digital modulation techniques and also for the different levels of jammer noise power. Under the multipath frequency-selective Rayleigh fading environment, the phase noise is estimated at the subblock level, which is further utilized to compensate the adverse effects of ICI by using the blindly estimated common phase error. For this processing, the blind phase noise compensation technique exploits the relationship between the calculated time-average values of the phase noise and the squared magnitude of channel-tap gain multiplied by the information symbols at each subcarrier.

The spreading of jammer noise with any probability density function over all subcarriers takes place due to the noise bucket effect, which reduces the impact of jammer noise power in the frequency-domain due to the discrete Fourier transform operation at the receiving end. It is evident from simulation results that the long OFDM symbol block period or the large number of subcarriers is beneficial in tackling the jammer noise plus additional white Gaussian noise (total noise), at the constant level of transmitted signal power and total noise. As the number of constellation points increases in the higher-order M-ary phase shift keying modulation techniques, the bit error rate performance gets deteriorated and the underlying OFDM system appears to be vulnerable to the adverse effects of jammer noise. Also, it is apparent from the presented results that the minimum mean square error detector shows marginally better performance than the zero forcing detector in the presence of jammer noise.

The practical systems usually do not have availability of the perfect channel state information at the wireless receiver. As a result, the receiving end is bound to include a channel estimator (generally adaptive in modern systems). This channel estimation may be imperfect due to the noisy environment and also in case of the time-varying channel characteristics. As the backbone of BPNC technique is the availability of perfect channel state information at the receiver, therefore future work includes the analysis of the impact of

imperfectly estimated channel state information [42], [43], [44], [45] on the BER performance of BPNC technique based OFDM systems, which use non-constant modulus modulation techniques.

## REFERENCES


[1] Marconi G. (1899). Wireless telegraphy, *Journal of the Institution of Electrical Engineers*, 28(139), 273-290.

[2] Bingham J.A.C. (1990). Multicarrier modulation for data transmission: an idea whose time has come, *IEEE Communications Magazine*, 28(5), 5-14.

[3] Weinstein S.B. and Ebert P.M. (1971). Data transmission by frequency-division multiplexing using the discrete Fourier transform, *IEEE Transactions on Communication Technology*, 19(5), 628-634.

[4] Henkel W. *et al.* (2002). The cyclic prefix of OFDM/DMT – an analysis, *International Zurich Seminar on Broadband Communications Access-Transmission-Networking* [4th: Zurich, Switzerland: 2002], pp. 22-1-22-3.

[5] R. W. Chang, U. S. Patent No. 3488445 A, 1970.

[6] Peled A. and Ruiz A. (1980). Frequency domain data transmission using reduced computational complexity algorithms, *IEEE International Conference on Acoustics, Speech and Signal Processing* [5th: Denver, Colorado, USA: 1980], pp. 964-967.

[7] Floch B.L., Lassalle R.H. and Castelain D. (1989). Digital sound broadcasting to mobile receivers, *IEEE Transactions on Consumer Electronics*, 35(3), 493–503.

[8] Reimers U. (1998). Digital Video Broadcasting, *IEEE Communications Magazine*, 36(6), 104-110.

[9] Egli J.J. (1957). Radio propagation above 40 MC over irregular terrain, *Proceedings of the IRE*, 45 (10), 1383-1391.

[10] Clarke R.M. (1968). A statistical theory of mobile radio reception, *The Bell System Technical Journal*, 47(6), 957-1000.

[11] Gans M.C. (1972). A power-spectral theory of propagation in the mobile radio environment, *IEEE Transactions on Vehicular Technology*, 21(1), 27-38.

[12] Hoffman D. and Karst O.J. (1975). The theory of Rayleigh distribution and some of its applications, *Journal of Ship Research*, 19(3), 172-191.

[13] Demir A., Mehrotra A. and Roychowdhury J. (2000). Phase noise in oscillators: a unifying theory and numerical methods for characterization, *IEEE Transactions on Circuits and Systems I: Fundamental Theory and Applications*, 47(5), 655-674.

[14] Armstrong J. (2009). OFDM for optical communications, *Journal of Lightwave Technol*ogy, 27(3), 189-204.

[15] Raniwala A. and Chiueh T. (2005). Architecture and algorithms for an IEEE 802.11-based multi-channel wireless mesh network, *Joint Conference of the IEEE Computer and Communication Societies* [24th: Miami, FL, USA: 2005], pp. 2223-2234.

[16] Meghwal P. and Sharma S. (2014). OFDM performance in an additive white Gaussian noise (AWGN) channel, *International Journal of Engineering and Technical Research*, 2(4), 174-176.

[17] Petrovic D., Rave W. and Fettweis G. (2005). Properties of the inter carrier interference due to phase noise in OFDM, *IEEE International Conference on Communications* [18th: Seoul, South Korea: 2005], pp. 2605-2610.

[18] Armada A.G. (2001). Understanding the effects of phase noise in orthogonal frequency division multiplexing (OFDM), *IEEE Transactions on Broadcasting*, 47(2), 153-159.

[19] Yi X. *et al.* (2016). Phase noise effects on phase-modulated coherent optical OFDM, *IEEE Photonics Journal*, 8(1), 1-8.

[20] Tomba L. (1998). On the effect of Wiener phase noise in OFDM systems, *IEEE Transactions on Commun*ications, 46(5), 580-583.

[21] Mathecken P.J. (2011). Performance analysis of OFDM with Wiener phase noise and frequency selective fading channel, *IEEE Transactions on Communications*, 59(5), 1321-1331.

[22] Pollet T., Bladel M.V. and Moeneclaey M. (1995). BER sensitivity of OFDM systems to carrier frequency offset and Wiener phase noise, *IEEE Transactions on Communications*, 43(2/3/4), 191-193.

[23] Moeneclaey M. (1997). The effect of synchronization errors on the performance of orthogonal frequency-division multiplexed (OFDM) systems, *Proceedings COST 254 Emerging Techniques for Communication Terminals* [Toulouse, France: 1997], pp. 1-5.

[24] Robertson P. and Kaiser S. (1995). Analysis of the effects of phase noise in orthogonal frequency division multiplexing (OFDM) systems, *IEEE International Conference on Communications* [8th: Seattle, WA, USA: 1995] pp. 1652-1657.

[25] Petrovic D. and Fettweis G. (2007). Effects of phase noise on OFDM systems with and without PLL: characterization and compensation, *IEEE Transactions on Communications*, 55(8), 1607-1616.

[26] Moose P.H. (1994). A technique for orthogonal frequency division multiplexing frequency offset correction, *IEEE Transactions on Communications*, 42(10), 2908-2914.

[27] Liu G. and Zhu W. (2007). Phase noise effects and mitigation in OFDM systems over Rayleigh fading channels, *Springer Wireless Personal Communications*, 41(2), 243-258.

[28] Wu S. and Bar-ness Y. (2002). A Phase Noise Suppression Algorithm for OFDM-based WLANs, *IEEE Communication Letters*, 6(12), 535-537.

[29] Gudmundson M. and Anderson P.O. (1996). Adjacent channel interference in an OFDM system, *IEEE Vehicular Technology Conference* [46th: Atlanta, GA, USA: 1996], pp. 918-922.

[30] Armstrong J. (1999). Analysis of new and existing methods of reducing intercarrier interference due to carrier frequency offset in OFDM, *IEEE Transactions on Communications*, 47(3), 365-369.

[31] Munier F., Eriksson T. and Svensson A. (2004). Receiver algorithms for OFDM systems in phase noise and AWGN, *IEEE International Symposium on Personal, Indoor and Mobile Radio Communication* [15th: Barcelona, Spain: 2004], pp. 1998-2002.

[32] Mir M.D. and Buttar A.S. (2015). Phase noise mitigation techniques in OFDM system: a survey, *IEEE International Conference on Electrical, Computer and Communication*

*Techologies* [2nd: Coimbatore, India: 2015], pp. 1-4.

[33] Piazzo L. and Mandarini P. (2002). Analysis of phase noise effects in OFDM modems, *IEEE Transactions on Communications*, 50(10), 1696-1705.

[34] Zou Q. and Sayed A.H. (2007). Compensation of phase noise in OFDM wireless systems, *IEEE Transactions on Signal Processing*, 55(11), 5407-5424.

[35] Sridharan G. and Lim T.J. (2010). Blind estimation of common phase error in OFDM and OFDMA, *IEEE Global Telecommunications Conference* [25th: Miami, FL, USA: 2010], pp. 1-5.

[36] Lee M.K., Yang K. and Cheun K. (2011). Iterative receivers based on subblock processing for phase noise compensation in OFDM systems, *IEEE Transactions on Communications*, 59(3), 792-802.

[37] Hossain M.A., Lin H. and Yamashita K. (2014). Low-complexity blind phase noise compensation in OFDM systems, *International Conference on Electrical Engineering and Information & Communication Technology* [1st: Dhaka, Bangladesh: 2014], pp. 1-4.

[38] Lee M.K., Lim S.C. and Yang K. (2012). Blind compensation for phase noise in OFDM systems over constant modulus modulation, *IEEE Transactions on Communications*, 60(3), 620-625.

[39] Suraweera H.A. and Armstrong J. (2004). Noise bucket effect for impulse noise in OFDM, *IEEE Electronics Letters*, 40(18), 1156-1157.

[40] Grover A., Kapoor D.S. and Kohli A.K. (2012). Characterization of impulse noise effects on space-times block-coded orthogonal frequency division multiplexing (OFDM) signal reception, *International Journal of Physical Sciences*, 4003-4011.

[41] Gong Y. and Hong X. (2009). OFDM joint data selection and phase noise cancellation for constant modulus modulations, *IEEE Transaction on Signal Processing*, 57(7), 2864-2868.

[42] Kapoor D.S. and Kohli A.K. (2015). Simulation of basis expansion model for channel fading using AR1 process, *Springer Wireless Personal Communnication*, 85(3), 791-798.

[43] Kohli A.K. and Kapoor D.S. (2015). Adaptive filtering techniques using cyclic prefix in OFDM systems for multipath fading channel prediction, *Springer Circuits, Systems, and Signal Processing*, 35(10), 3595-3618.

[44] Bansal A. and Kohli A.K. (2016). Suppression of impulsive noise in OFDM system using imperfect channel state information, *International Journal for Light and Electron Optics*, 127(4), 2111-2115.

[45] Sehrawat S. and Kohli A.K. (2016). Optimized mitigation of impulsive noise in OFDM system using CSI, *International Journal for Light and Electron Optics*, 127(20), 9627-9634.

[46] Papoulis A., *Probablility, Random Variables, and Stochastic Processes*. 2nd ed. McGraw-Hill: New York, 1991.

# APPENDIX A
# STATISTICS OF TOTAL NOISE IN OFDM SYSTEMS

The total noise in OFDM system at the *k*th subcarrier can be represented as

$$Tn_k = \overline{W\Lambda}_k, \tag{A.1}$$

$$= W_k + \Lambda_k, \qquad 0 \le k \le N-1 \tag{A.2}$$

where, $N$ is the number of subcarriers, $W_k$ is the normalized $N$-point DFT coefficient of $\left\{\exp\left(j\left(\Phi_i^R - \Phi_i\right)\right)w_i\right\}_{i=0}^{N-1}$ and $\Lambda_k$ is the normalized $N$-point DFT coefficient of $\left\{\exp\left(j\left(\Phi_i^R - \Phi_i\right)\right)\eta_i\right\}_{i=0}^{N-1}$. Here, $\Phi_i^R$ and $\Phi_i$ represent the residual phase noise after intercarrier interference mitigation and Wiener phase noise respectively. $w_i$ represents the additive-white-Gaussian-noise (AWGN) and $\eta_i$ denotes jammer noise at time instant *i*. Both $W_k$ and $\Lambda_k$ are approximated as Gaussian distributed random-variables (RVs). $W_k$ is Gaussian random variable with zero-mean and variance $\sigma_w^2$, while $\Lambda_k$ is a Gaussian random variable with zero-mean and variance $\sigma_\eta^2$.

The AWGN component and the jammer noise at the *k*th subcarrier are independent random variables, which means that the value of one random variable cannot be used to estimate the nature or value of the other random variable. In this case, the jammer noise may be more than the additive white Gaussian noise.

The mean or the expected value of the total noise at the *k*th subcarrier i.e., $Tn_k$ can be calculated as [46],

$$E\left[Tn_k\right] = E\left[W_k + \Lambda_k\right], \tag{A.3}$$

$$= E\left[W_k\right] + E\left[\Lambda_k\right], \qquad 0 \le k \le N-1 \tag{A.4}$$

where, $E\left[.\right]$ represents expectation operator. As it has been already stated that the $W_k$ and $\Lambda_k$ are Gaussian distributed random variable with zero-mean implying that $E\left[W_k\right] = 0$ and $E\left[\Lambda_k\right] = 0$. It follows that

$$E\left[Tn_k\right]=0, \tag{A.5}$$

The variance of the total noise in OFDM symbol block at the *k*th subcarrier i.e., $\sigma_{Tn}^2$ can be evaluated in a similar way as follows

$$\text{var}\left[Tn_k\right]=\sigma_{Tn}^2=E\left[\left\{Tn_k-E\left(Tn_k\right)\right\}^2\right], \tag{A.6}$$

$$=E\left[\left\{\left(W_k+\Lambda_k\right)-E\left(W_k+\Lambda_k\right)\right\}^2\right], \tag{A.7}$$

$$=E\left[\left\{W_k+\Lambda_k-E\left(W_k\right)-E\left(\Lambda_k\right)\right\}^2\right], \tag{A.8}$$

$$=E\left[\left[\left\{W_k-E\left(W_k\right)\right\}+\left\{\Lambda_k-E\left(\Lambda_k\right)\right\}\right]^2\right], \tag{A.9}$$

$$=E\left[\left\{W_k-E\left(W_k\right)\right\}^2+\left\{\Lambda_k-E\left(\Lambda_k\right)\right\}^2+2\left\{W_k-E\left(W_k\right)\right\}\left\{\Lambda_k-E\left(\Lambda_k\right)\right\}\right], \tag{A.10}$$

$$\sigma_{Tn}^2=E\left[\left\{W_k-E\left(W_k\right)\right\}^2\right]+E\left[\left\{\Lambda_k-E\left(\Lambda_k\right)\right\}^2\right]+2E\left[\left\{W_k-E\left(W_k\right)\right\}\left\{\Lambda_k-E\left(\Lambda_k\right)\right\}\right], \tag{A.11}$$

Since, $W_k$ and $\Lambda_k$ are independent RVs, it means that $W_k-E\left[W_k\right]$ and $\Lambda_k-E\left[\Lambda_k\right]$ are also independent RVs. This implies that

$$E\left[\left\{W_k-E\left(W_k\right)\right\}\left\{\Lambda_k-E\left(\Lambda_k\right)\right\}\right]=E\left[W_k-E\left(W_k\right)\right]E\left[\Lambda_k-E\left(\Lambda_k\right)\right], \tag{A.12}$$

The variance of random variables $W_k$ and $\Lambda_k$ can be expressed as

$$\sigma_w^2=E\left[\left\{W_k-E\left(W_k\right)\right\}^2\right], \tag{A.13}$$

$$\sigma_\eta^2=E\left[\left\{\Lambda_k-E\left(\Lambda_k\right)\right\}^2\right], \tag{A.14}$$

On simplifying Equations (A.11) - (A.14), we obtain

$$\sigma_{Tn}^2=\sigma_w^2+\sigma_\eta^2+2E\left[\left\{W_k-E\left(W_k\right)\right\}\right]E\left[\left\{\Lambda_k-E\left(\Lambda_k\right)\right\}\right], \tag{A.15}$$

$$\sigma_{Tn}^2=\sigma_w^2+\sigma_\eta^2+2\left\{E\left(W_k\right)-E\left[E\left(W_k\right)\right]\right\}\left\{E\left(\Lambda_k\right)-E\left[E\left(\Lambda_k\right)\right]\right\}, \tag{A.16}$$

where, $E\left[E\left(W_k\right)\right]$ is equal to $E\left[W_k\right]$ and $E\left[E\left(\Lambda_k\right)\right]$ is equal to $E\left[\Lambda_k\right]$. It follows that

$$\sigma_{Tn}^2 = \sigma_w^2 + \sigma_\eta^2 + 2\left\{E\left(W_k\right) - E\left(W_k\right)\right\}\left\{E\left(\Lambda_k\right) - E\left(\Lambda_k\right)\right\}, \tag{A.17}$$

$$\sigma_{Tn}^2 = \sigma_w^2 + \sigma_\eta^2 + 2\left(0\right)\left(0\right), \tag{A.18}$$

$$\sigma_{Tn}^2 = \sigma_w^2 + \sigma_\eta^2, \tag{A.19}$$

Hence, we may infer that the total noise in the OFDM system is also Gaussian distributed with zero-mean and its variance is equal to the sum of the variance of the AWGN component and variance of jammer noise i.e., $\sigma_w^2 + \sigma_\eta^2$.

## LIST OF PUBLICATIONS

[1] Sandhu J.P.K. and Kohli A.K. (2017). Impact of jammer noise on blind phase noise compensation in OFDM systems, *International Journal for Light and Electron Optics*, under review.